HSPF Watershed Model Update and Calibration Report for the Duluth Urban Area

September 22, 2022

PREPARED FOR

Minnesota Pollution Control Agency
520 Lafayette Road
St. Paul, MN 55155

PREPARED BY

Tetra Tech, Inc.
One Park Drive, Suite 200
PO Box 14409
Research Triangle Park, NC 27709
Tel 919-485-8278

wq-iw10-11o

TABLE OF CONTENTS

LIST OF FIGURES

LIST OF TABLES

ACRONYMS/ABBREVIATIONS

Acronyms/Abbreviations	Definition
1W1P	One Watershed, One Plan
CASTNET	Clean Air Status and Trends Network
DOC	Dissolved Organic Carbon
DSN	Data Series Number
EIA	Effective Impervious Area
ET	Evapotranspiration
GIS	Geographic Information System
HRU	Hydrologic Response Unit
HSG	Hydrologic Soil Group
HSPF	Hydrologic Simulation Program FORTRAN
HUC	Hydrologic Unit Code
IMPLND	Impervious Land Unit
MIA	Mapped Impervious Area
MPCA	Minnesota Pollution Control Agency
NADP	National Atmospheric Deposition Program
NCDC	National Climatic Data Center
NCEP	National Centers for Environmental Protection
NLCD	National Land Cover Database
NLDAS-2	North American Land Data Assimilation System
NRRI	Natural Resources Research Institute
NSE	Nash Sutcliffe Efficiency
NSIDC	National Snow and Ice Data Center
NWI	National Wetland Inventory
PERLND	Pervious Land Unit
PET	Potential Evapotranspiration
PRISM	Parameter-elevation Relationships on Independent Slopes Model
RE	Relative Error
RQUAL	Reach Quality Module
SNODAS	Snow Data Assimilation System
SSEBop	Simplified Surface Energy Balance
SWE	Snow Water Equivalent
TIA	Total Impervious Area
TMDL	Total Maximum Daily Load
TOC	Total Organic Carbon
TSS	Total Suspended Solids
USGS	United States Geological Survey

Acronyms/Abbreviations	Definition
WDM	Watershed Data Management
WLSSD	Western Lake Superior Sanitary District
WRAPS	Watershed Restoration and Protection Strategies
WY	Water Year

1.0 INTRODUCTION

This report describes the update and recalibration of a Hydrologic Simulation Program – FORTRAN (HSPF; Bicknell et al., 2014) model of Duluth urban area in northeastern Minnesota (Figure 1-1 and Figure 1-2). The previous HSPF model was developed and calibrated to simulate conditions through 2016 (Tetra Tech, 2019) to support the development of Watershed Restoration and Protection Strategies (WRAPS). The Duluth WRAPS modeling project was initiated to provide a finer-scale HSPF model for the developed areas in order to better simulate stormwater and urban conditions in the highly developed environment of Duluth and surrounding areas. This report discusses the extension of the Duluth urban area model through Water Year (WY) 2021, updates to model land use/cover using more recent data, and the subsequent recalibration of hydrology and water quality.

The modeled area covers approximately 140.6 square miles of St. Louis and Lake Counties in northeast Minnesota, and includes developed areas within Duluth, Hermantown, Proctor, and surrounding rural land. The majority of the study area is composed of small creeks and rivers draining to the St. Louis River Estuary and directly to Lake Superior. A small catchment draining to Wild Rice Lake to the northwest is also included in the model to represent runoff from Duluth International Airport. Larger subwatersheds include (from south to north) Mission Creek, Kingsbury Creek, Keene Creek, Miller Creek, Chester Creek, Tischer Creek, Amity Creek, and Lester River. Fourteen of the named streams in the area are designated trout streams: Mission, Stewart, Sargent, Knowlton, Kingsbury, Merritt, Keene, Coffee, Buckingham, Miller, Chester, Tischer, Amity, and Lester.

This effort was completed because the Minnesota Pollution Control Agency (MPCA) works to keep models of watersheds in the state up-to-date so the models remain viable tools for planning. Under Minnesota's Watershed Approach, HSPF models are used to support the development of WRAPS reports, Comprehensive Watershed Management Plans (One Watershed, One Plan; 1W1P), and Total Maximum Daily Loads (TMDL). MPCA's HSPF models are designed to support biological stressor identification and analysis of pollutant-related impairments. In addition, the work was completed in anticipation of using the updated and recalibrated model to support development of a mercury TMDL for the St. Louis River Estuary and Harbor.

A watershed model is a tool to aid understanding of processes and consequences of human activities in a river basin, however, it is only one among a variety of tools. A watershed model is not a substitute for direct monitoring of physical and biological conditions in streams and lakes. When properly calibrated to represent observations, a model can, however, provide a reasonable mechanism for the extrapolation of monitoring data in space (to unmonitored locations) and in time (to unmonitored or future time periods). A watershed model also enables experiments to investigate how changes (such as changes in land use, management practices, or climate) may affect conditions in the watershed and allow policymakers and stakeholders to plan accordingly. To be useful for these purposes the credibility of the model (and its associated level of uncertainty) must be established through comparison to real world data, preferably collected in the modeled drainage area, and through local partner input, as described in this report.

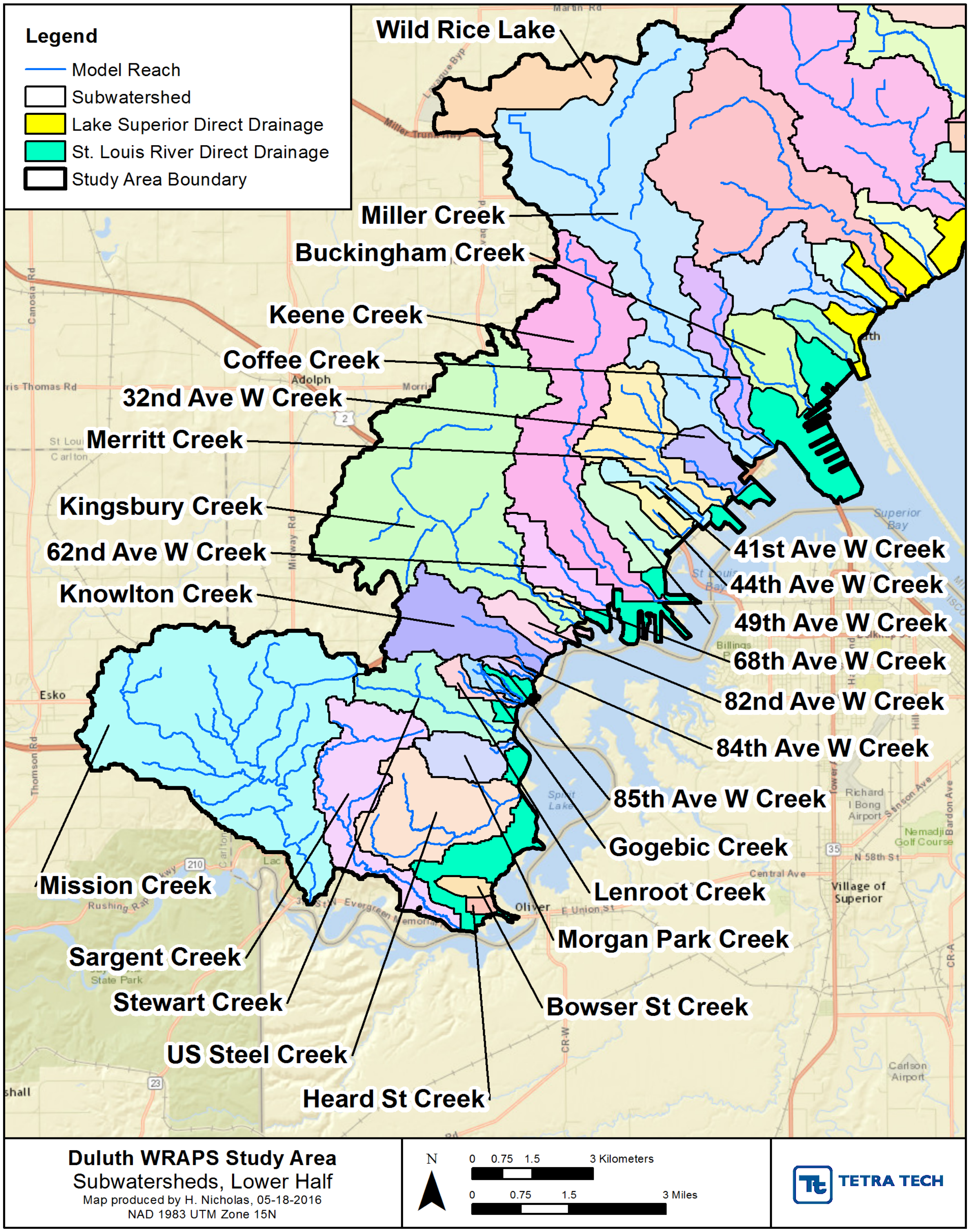

Figure 1-1. Duluth urban area HSPF model (lower half)

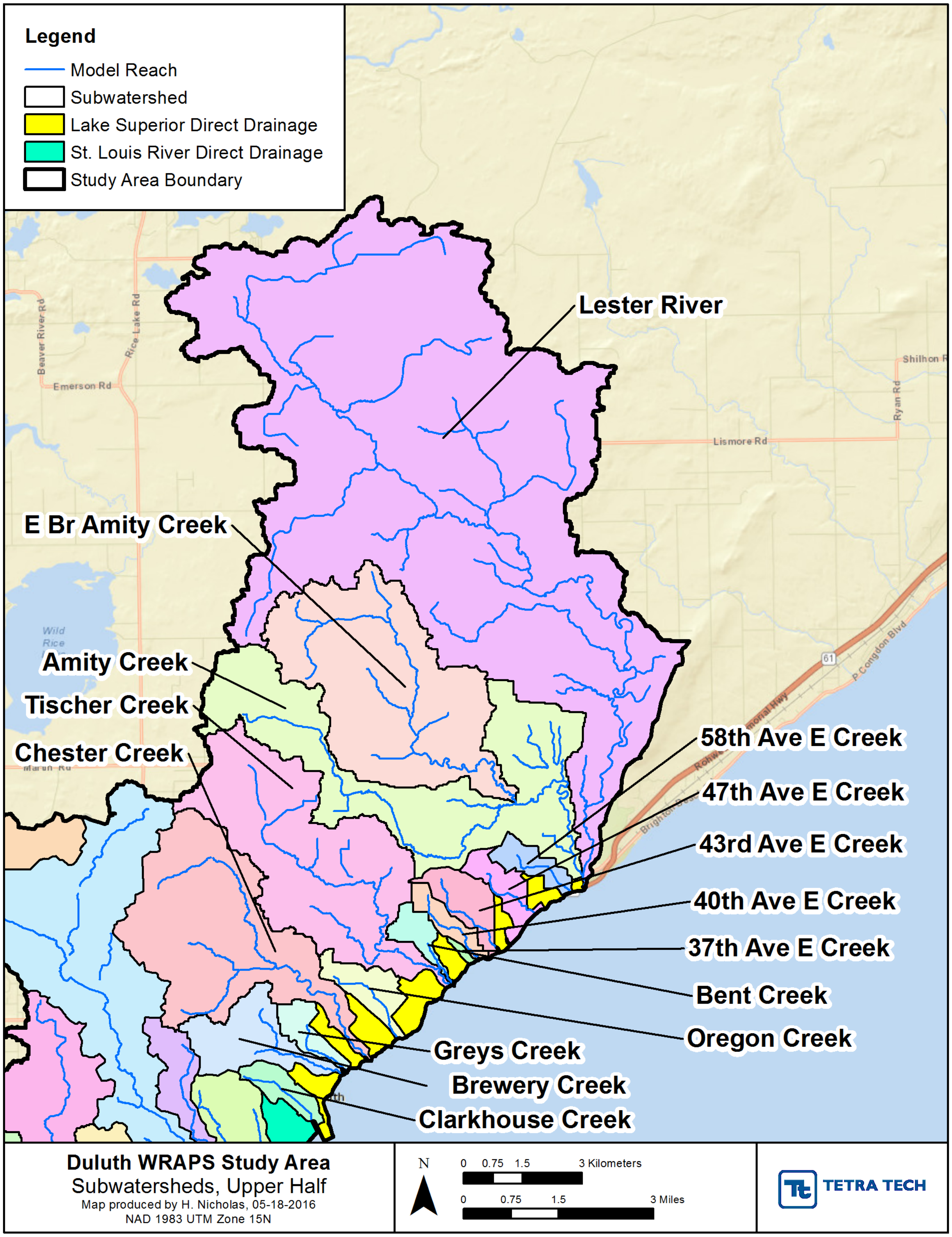

Figure 1-2. Duluth urban area HSPF model (upper half)

2.0 MODEL EXTENSION AND UPDATE

The simulation period of the Duluth urban area HSPF model was extended through WY 2021. Model input time series for weather and atmospheric deposition were extended as discussed in Sections 2.1 and 2.3, respectively. In addition, more recent land use/cover data were incorporated into the model as described in Section 2.2. No permitted point sources (e.g., wastewater treatment plants) discharge to these streams so no point source input time series needed to be extended as part of this effort. Delineations, stream routing, hydraulic/channel geometric properties, and other aspects of the model structure were maintained from the previous version for this iteration.

2.1 WEATHER

Weather data are one of the most important inputs for continuous simulation models. The ability of a model to predict hydrologic response and pollutant generation, fate, and transport is strongly influenced by the accuracy and appropriate representation of meteorological data. This is a particularly important issue for a fine-scale model of Duluth streams where there can be substantial variability in microclimate based on elevation and proximity to Lake Superior. Meteorological data required for a HSPF model consists of hourly precipitation (PREC), air temperature (ATEM), cloud cover (CLOU), dew point temperature (DEWP), solar radiation (SOLR), wind speed (WIND) and evapotranspiration (PEVT). Several data sources were reviewed during the previous Duluth HSPF modeling effort to determine the most optimal way to represent meteorology in the Duluth WRAPS study area. Data sources selected to represent meteorology in the Duluth HSPF model include:

- Local precipitation data from Western Lake Superior Sanitary District (WLSSD) collected on an hourly basis, generally available beginning in 2002 or 2006
- Meteorological data distributed by the National Climatic Data Center (NCDC)
- Meteorological data produced by the Parameter-elevation Regressions on Independent Slopes Model (PRISM), which provides interpolated gridded data for the entire contiguous United States
- Hourly gridded meteorological data produced by the North American Land Data Assimilation System (NLDAS-2)

PRISM provides annual, monthly, and daily gridded precipitation data for the conterminous United States (Daly et al., 2008, 2015; daily output was added to PRISM in 2015). PRISM calculates a climate-elevation regression function for each grid cell and the regression is used to distribute station-based precipitation data to the grid cell. Approximately 13,000 precipitation stations are used in the analysis. For each grid cell, precipitation stations are assigned weights based on location, elevation, coastal proximity, topographic facet orientation, vertical atmospheric layer, topographic position, and orographic effectiveness of the terrain; the stations are then entered into the regression function to establish the gridded precipitation product.

NLDAS-2 is another gridded meteorological time-series (Mitchell et al., 2004). NLDAS-2 (http://ldas.gsfc.nasa.gov/nldas/NLDAS2forcing.php) provides continuous hourly data from 1979 to present on a 1/8-degree grid that has been processed to fill gaps. The precipitation data in NLDAS-2 are based on interpolation of daily precipitation including orographic adjustments based on PRISM and temporally disaggregated using Doppler radar and satellite data. NLDAS-2 also provides solar radiation, wind at 10 m (which can be scaled to wind at 2 m), and absolute humidity plus air pressure, from which dew point can be calculated. Cloud cover (which is only needed to estimate long wave radiation exchange with the atmosphere) is not included in the NLDAS output, but can be back-calculated from the ratio of estimated incident solar radiation to cloud free solar radiation during daylight hours using the regression relationship developed by Davis (1996).

In the previous Duluth HSPF model that ran from 10/1/1993 to 12/31/2016, gridded daily precipitation totals from PRISM were disaggregated to hourly values using local NCDC and WLSSD weather station data (i.e., patterns), and Tetra Tech repeated this effort when extending the model time period through water year (WY) 2021. The best source of hourly precipitation data in the study area is the NCDC station at Duluth International Airport. However, there are spatial variations in precipitation patterns across the study area that cannot be accounted for using a single station. The WLSSD precipitation monitoring network therefore was used to enhance the hourly disaggregation of daily PRISM values. The WLSSD data were processed by identifying gaps in monitoring and filling data gaps with the nearest other station's data adjusted using a station-specific long-term precipitation ratio. Upon review of the previous model period's PRISM grid cell alignment, we noticed that the grids had been shifted by one cell to the left, so the previous disaggregation template was re-applied to corrected PRISM grid cell data for the entire simulation period.

The meteorological datasets for precipitation are shown in Figure 2-1. The WLSSD and NCDC hourly data stations are shown as green triangles. PRISM grid cells are shown with red outline and are color-coded according to their assignment to hourly disaggregation source. The grid cell assignment is largely influenced by distance from the lake. Daily precipitation in each PRISM grid cell was disaggregated to hourly values using the assigned weather station, with temporal adjustments to account for time zone differences between local data and PRISM (which uses 1200 UTC as the beginning of its day). Unique hourly precipitation time series were developed for each of the 36 PRISM grid cells as a result. For modeling purposes, each grid cell was assigned its PRISM code as the weather region identifier used in input files and subsequent documentation. The weather region IDs are shown within each cell in the figure.

PRISM also provides daily minimum and maximum air temperature. For the previous modeling period, long-term hourly air temperature data were only available from the NCDC station at Duluth International Airport, so that station was used to develop the hourly air temperature pattern for each PRISM grid cell. Other meteorological time series (cloud cover, dew point temperature, and wind speed) were available from the Duluth Airport station and were used for the entire modeling area, which was repeated for the model extension period through 9/30/2021. Data gaps present in the extended cloud cover, dew point temperature, and wind speed time series were filled using an interpolation strategy as these were relatively short. Solar radiation was not available for the extension period from the Duluth Airport station, so solar radiation was obtained via the NLDAS-2 meteorological time-series (Mitchell et al., 2004). To be consistent with data acquisition and solar radiation representation in the updated HSPF model, the solar radiation time series was replaced for the entire modeling period.

The remaining weather parameter, potential evapotranspiration (PET), was estimated uniquely for each of the 36 (PRISM) weather regions using the Penman Pan method (Penman, 1948; Kohler et al, 1955) for the previous simulation time period, and that method was extended to the updated time-series as well. This Penman Pan evapotranspiration method includes air temperature, dew point/humidity, solar radiation, and wind travel as inputs, and the latter three were derived from the Duluth International Airport weather station. Daily minimum and maximum PRISM air temperature series were used in the calculation of PET, allowing for spatial variation.

Meteorological data from PRISM, NLDAS, NCDC and WLSSD were used to extend the hourly weather forcing series. The basic overview of each meteorological input, data source, and processing notes are provided in Table 2-1. The Gridded Weather Data Processing Tool (MetTool), developed by Tetra Tech for MPCA, was used to download and extract gridded data for the model (Tetra Tech ,2020).

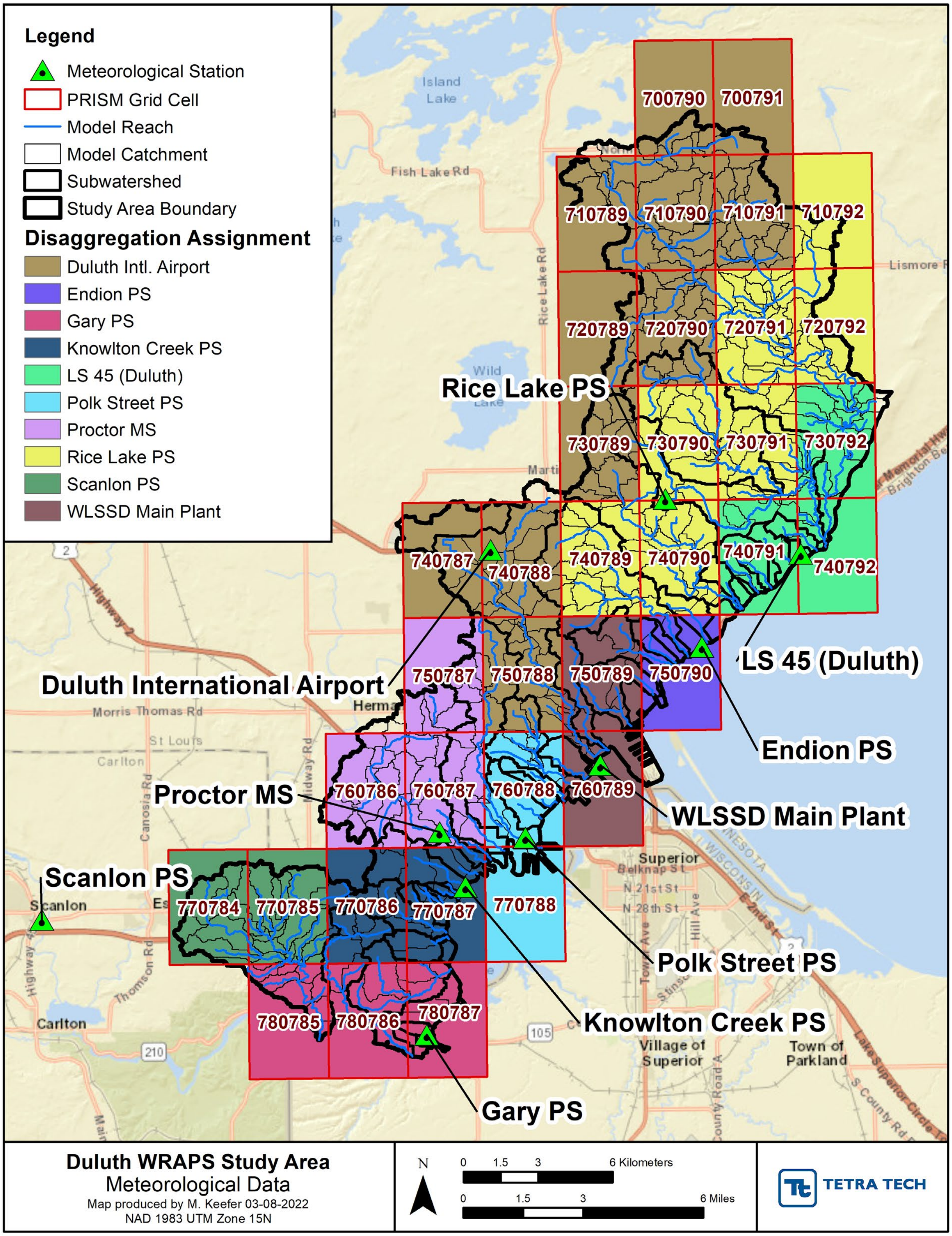

Figure 2-1. Meteorological data sources for the Duluth urban area HSPF model update

Table 2-1. Summary of HSPF meteorological input time series

HSPF Model Input	Description (units)	Parameter Source	DSNs in the WDM	Processing Notes
PREC	Precipitation (in)	PPT (PRISM), APCP (NLDAS), P01I (NCDC), PRECIP (WLSSD)	101-136	Daily PRISM precipitation data are primarily disaggregated using hourly gap-filled NCDC/WLSSD precipitation data Daily PRISM precipitation data are disaggregated using NLDAS hourly patterns or the random cascade method when PRISM precipitation is nonzero and the NCDC/WLSSD station was zero
ATEM	Air Temperature (°F)	TMP (NLDAS), TMPF (NCDC)	301-336	Hourly air temperature pattern developed using NCDC Duluth International Airport station data and interpolated for each PRISM grid cell between daily minimum and maximum air temperature values
SOLR	Solar Radiation (Ly)	DSWRF (NLDAS)	505	Hourly short-wave radiation, used directly for PRISM grid cell 740788, aligning with the Duluth International Airport
CLOU	Cloud Cover (tenths; 0-10)	SKYC1 (NCDC)	405	Translated hourly NCDC Duluth International Airport station cloud cover codes to numeric values
DEWP	Dew Point Temperature (°F)	DWPF (NCDC)	805	Hourly dewpoint temperature, used directly from NCDC Duluth International Airport station and gap-filled with interpolation strategy
WIND	Wind Travel (mi)	SKNT (NCDC)	605	Hourly wind travel, used directly from NCDC Duluth International Airport station and gap-filled with interpolation strategy
PEVT	Potential Evapotranspiration (in)	TMP (NLDAS), DSWRF, TMPF, SKNT, DWPF (NCDC)	201-236	Computed from solar radiation, air temperature, wind travel, and dew point temperature

Note: All series were converted to HSPF compatible units.

2.2 LAND USE/COVER

The HSPF model is constructed using a combination of land use and land cover to represent characteristics of urban and rural landscapes in the Duluth area. In general, the land cover indicates the physical land type and land use refers to how a piece of land is used or managed. The combination of land use and land cover provides comprehensive information about previous and impervious surfaces that are needed by the HSPF model for hydrological and water quality simulations. The land use in the model is based primarily on data provided by the City of Duluth, which includes a parcel GIS database and a right-of-way GIS database. The parcel database includes a detailed description of the primary land use of each polygon, as well as other information. The land use classes are simplified and grouped into roads, residential, developed (low, high, and medium), undeveloped, and Carlton County classes for the HSPF modeling (Figure 2-2); for details see the previous Tetra Tech (2019) report. Parcel data information from the earlier version of the model was maintained for this iteration.

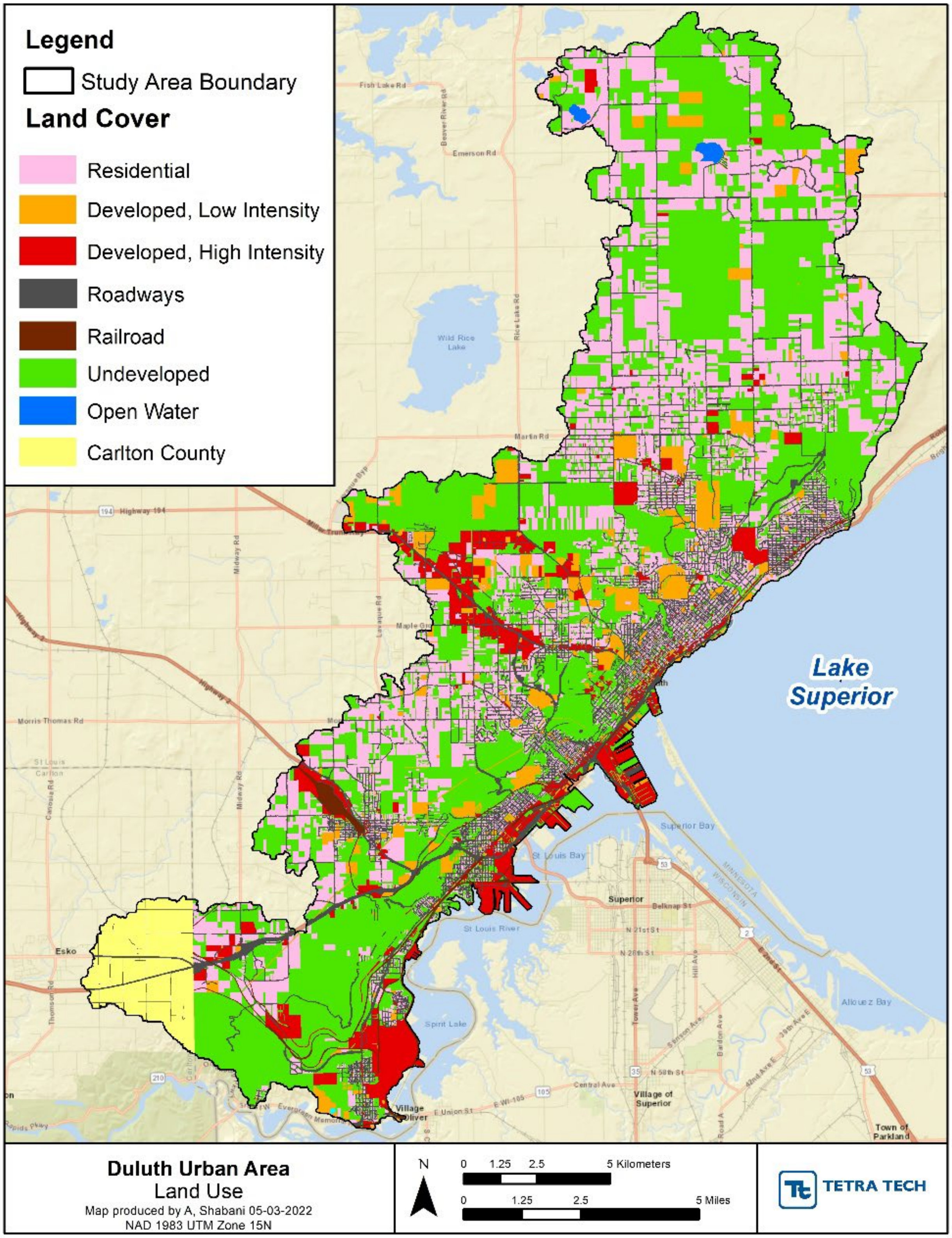

Figure 2-2. Land use in Duluth urban area HSPF model

The land cover for the Duluth model was originally developed using the National Land Cover Database (NLCD) 2011, LANDFIRE 2011, and a GIS wetlands inventory layer prepared by the Natural Resources Research Institute (NRRI) of the University of Minnesota, Duluth (Tetra Tech, 2019). To account for changes in land cover due to natural forces and anthropogenic activities, more recent land cover information was incorporated into the model. NLCD 2016 land cover was downloaded and compared to NLCD 2011 to identify changes in the drainage area overtime. The changes were estimated to be small (2.4 percent of the total watershed area) and fairly distributed across the study area (Figure 2-3). For these areas, the model land cover was updated using NLCD 2016. Figure 2-4 shows distribution of land covers in Duluth area. The rock outcrop locations for the model are defined using data from the Minnesota Geological Survey (University of Minnesota, 2019) and these areas were maintained. The land cover and land use layers for the watershed were overlaid and combined using ArcGIS 10.8 program to develop the Hydrological Response Units (HRUs) for the model. A HRU is the fundamental spatial unit of the HSPF model and it represents a unique combination of land features.

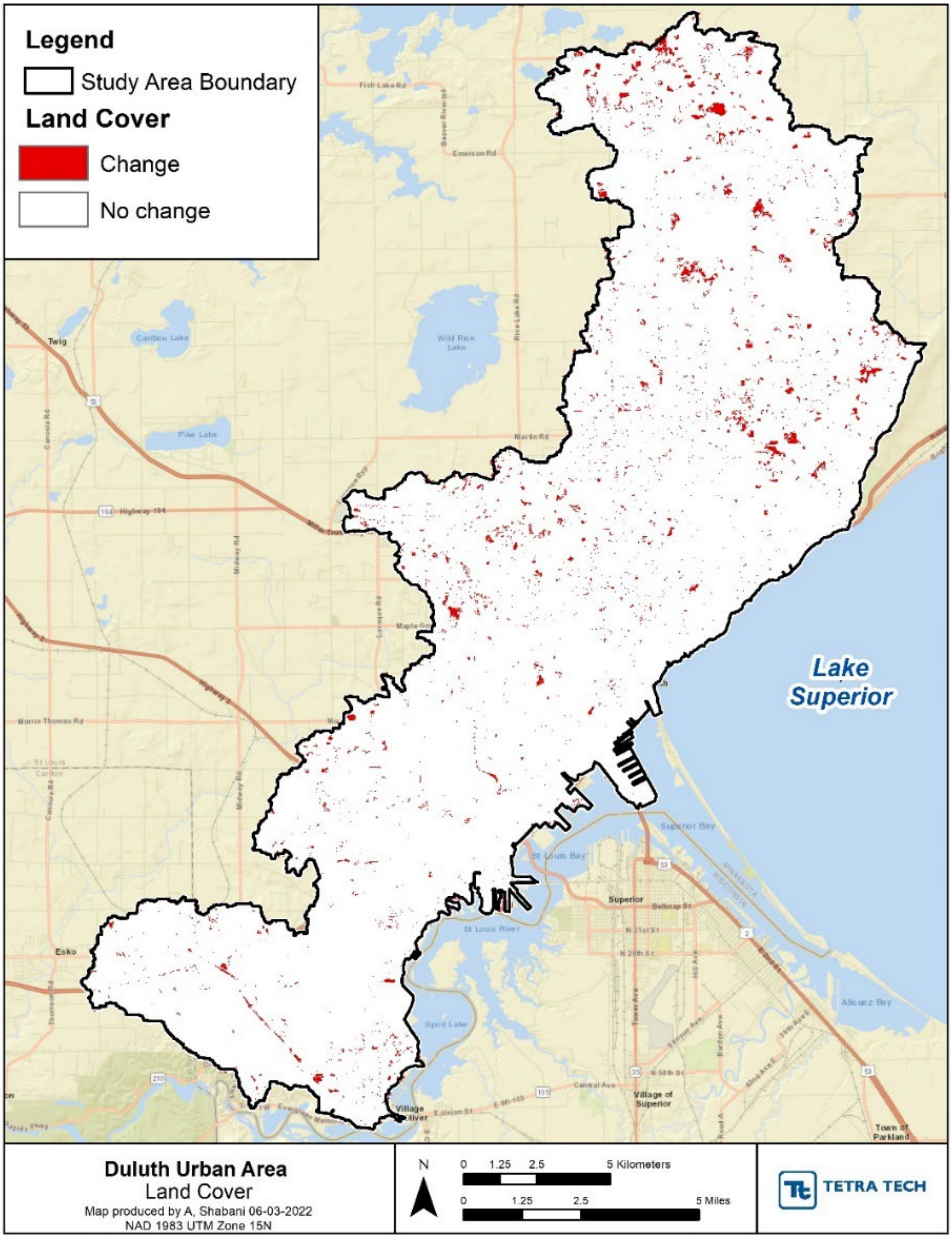

Figure 2-3. Change in land cover classification from NLCD 2011 and 2016

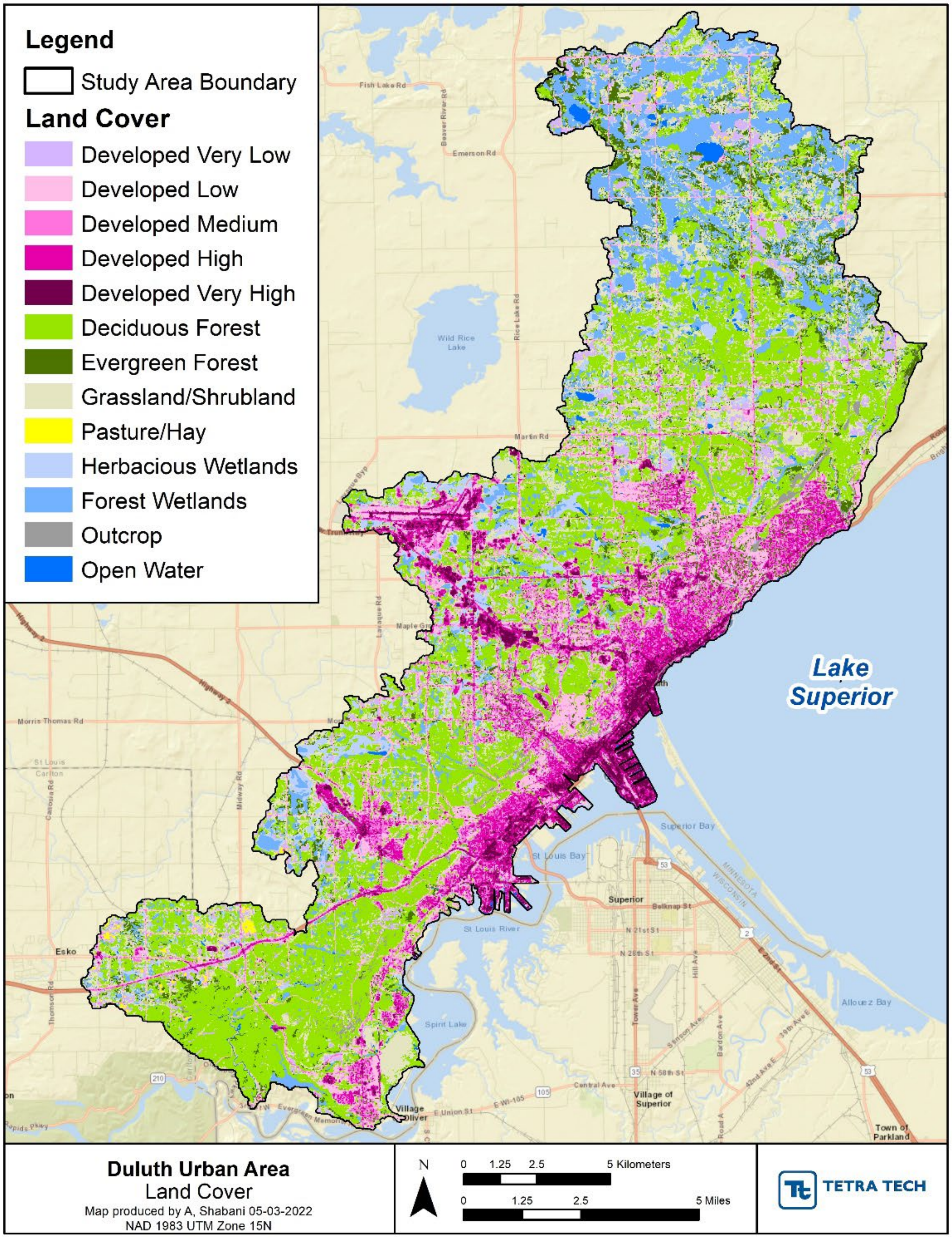

Figure 2-4. Duluth urban area land cover and use

HRUs were developed consistent with the methods outlined in Tetra Tech (2019). Most soils in Duluth area have a very low inflation rate (or high potential runoff) and are classified as Hydrologic Soil Group (HSG) D. Separation into soil classes was deemed not necessary because the soil information is largely redundant with the land use and land cover classes in this setting. The HRUs in the Duluth HSPF model, therefore, are a combination of land use and land cover, plus weather zone.

In the HSPF model, HRUs are classified into PERLND and IMPLND land segments to represent pervious and impervious surfaces, respectively. Pervious and impervious classes in the new model are the same as the older model and were assigned as described in the Tetra Tech (2019) model report (Table 2-1). The HRU pervious classes for the study area are presented in Figure 2-5. Each model HRU has a three-digit numeric code used within the HSPF model. In the Duluth model, the first two numbers indicate the HRU base category and weather regions are assigned to HRUs by adding a multiple of 20 to the numeric code, separately for each weather region. For instance, HRU number 101 represents the deciduous forest in weather zone (PRISM cell) 700790, and HRU number 121 represents the deciduous forest in weather zone (PRISM cell) 700791.

Impervious surfaces accelerate surface runoff generation by reducing infiltration of the soil surface layer. Total impervious area (TIA) or mapped impervious area (MIA) is frequently used in rainfall-runoff simulation to calculate impacts of developed/urban lands. Studies have shown that effective impervious area (EIA), or a portion of total impervious area that is hydraulically connected to the storm sewer system is a better parameter for runoff simulation in urban areas (Ebrahimian and Wilson, 2015). EIA is usually reported as a percentage of the total basin and subbasin and it is smaller than TIA, except in highly urbanized basins where EIA could be equal to TIA. The NLCD 2016 30 m impervious coverage was used to calculate the percentage of MIA within the model HRUs. Sutherland EIA equation for the average basin (Equation 1, Sutherland, 1995) was applied to calculate EIA from MIA:

$$EIA = 0.1 \times (MIA)^{1.5} \quad for\ MIA \geq 1 \quad (1)$$

The area of IMPLND for each HRU was then calculated by multiplying EIA and HRU area, and the PERLND area was calculated by subtracting the IMPLND area from the total HRU area.

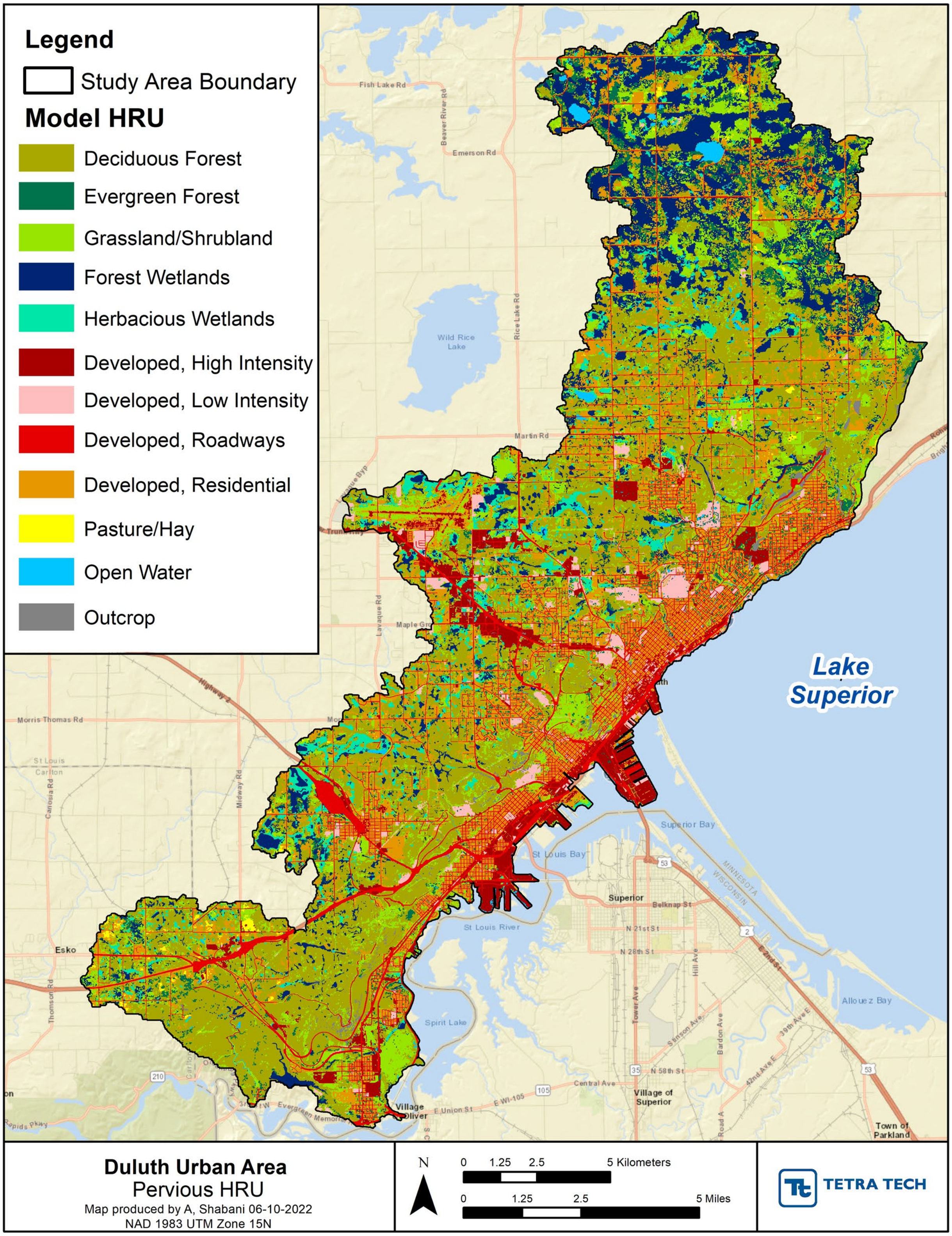

Figure 2-5. Duluth HSPF model HRUs

2.3 ATMOSPHERIC DEPOSITION

The HSPF model simulates wet and dry deposition of ammonia-N and nitrate-N to pervious surfaces, impervious surfaces, and waterbodies as well as the wet and dry deposition of phosphorus direct to the model reaches. Atmospheric deposition of phosphorus to the uplands is not simulated because it is implicit in the sediment potency representation of pervious land loading and the buildup/washoff representation of impervious land loading of phosphorus.

Wet deposition concentrations of ammonia and nitrate N (as mg/L) are derived from seasonal data recorded at National Atmospheric Deposition Program (NADP) station MN16 (Marcell Experimental Forest) because other NADP stations near Duluth either did not become operational until 1997 or ended prior to 2012 and thus do not cover the full time span of the model. Previous Tetra Tech work extended the deposition time series through 2014. To extend the HSPF model to current conditions, Tetra Tech downloaded the seasonal wet deposition concentrations of ammonia and nitrate N for the NADP MN16 monitoring station, converted to concentrations as N, and extended the model time series through the fall 2021 season (new model end date of 9/30/2021).

The Clean Air Status and Trends Network (CASTNET) monitors the dry deposition of ammonia and nitrate. Dry deposition rates of ammonia and nitrate N (as lb/ac) are taken from CASTNET monitoring. There are no CASTNET stations within or particularly close to Duluth, so Tetra Tech used the station at Voyageurs National Park (VOY413) for the period after 1996, filling earlier dates with monitoring from Perkinstown, WI (PRK134). Where data gaps existed in the VOY413 seasonal time series, monitoring data from PRK134 was used to gap fill missing dates with a long-term ratio of VOY413 to PRK134 data. Seasonal dry deposition rates (lb/acre) of ammonia and nitrate from the VOY413 and PRK134 monitoring stations were converted to mass fluxes of N (i.e., lb-N/acre) for use in the HSPF model. The CASTNET dry deposition rate time series of ammonia and nitrate were extended to the fall 2021 season.

After downloading the NADP wet deposition concentration and CASTNET dry deposition flux data and extending the time series, time series plots were created and reviewed for quality assurance. Figure 2-6 portrays the trend in wet atmospheric deposition over time, and Figure 2-7 shows trends in dry deposition flux over the extended 1/1/1993 to 9/30/2021 model time period. After the review, the seasonal time series were converted to monthly format and imported to a model WDM file for use in the HSPF model.

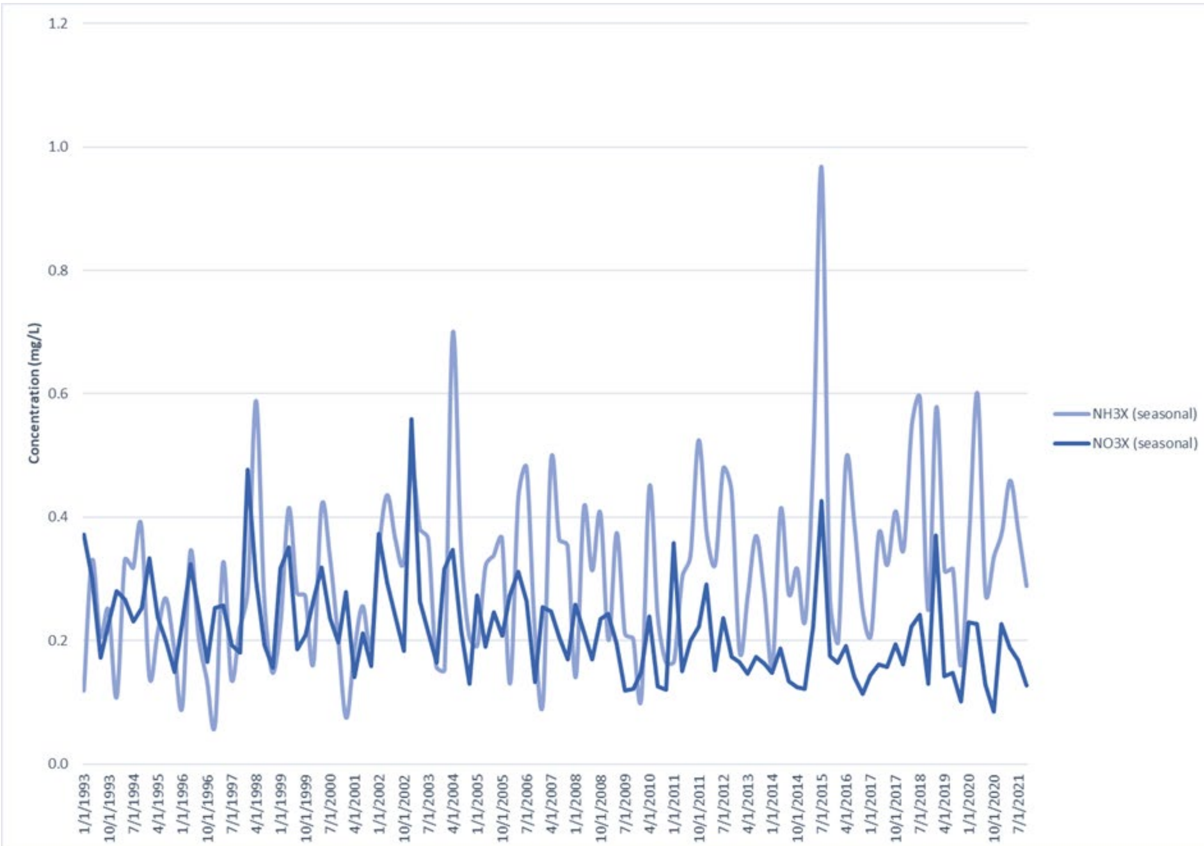

Figure 2-6. HSPF model time series plot for wet deposition concentrations (NH3 and NO3)

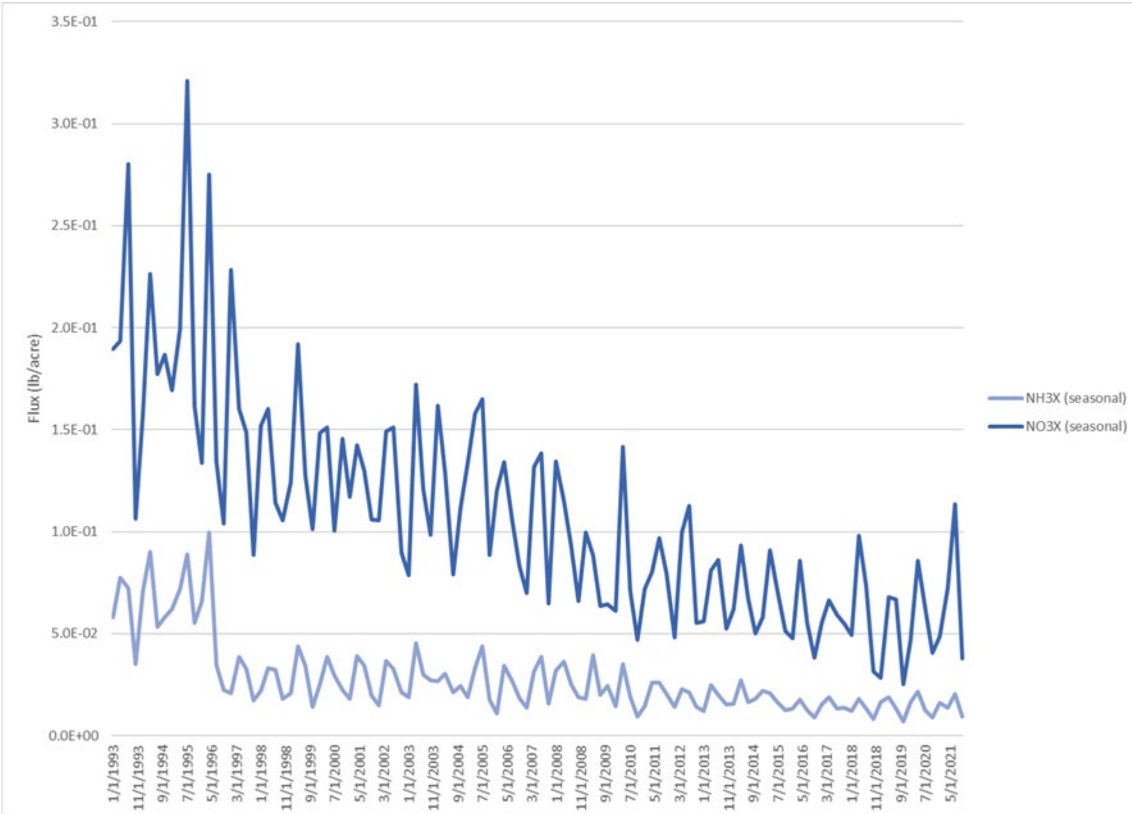

Figure 2-7. HSPF model time series plot for dry deposition flux (NH3 and NO3)

3.0 HYDROLOGIC CALIBRATION AND VALIDATION

3.1 APPROACH

The level of performance and overall quality of the hydrologic calibration is evaluated in a weight of evidence approach that includes both visual comparisons and quantitative statistical measures. The calibration proceeds in a sequential, yet often iterative, manner through (1) general representation of the overall water balance, (2) calibration of snow accumulation and melt, (3) assurance of consistency with satellite-based estimates of actual ET, and (4) detailed calibration relative to flow gaging records for seasonal flows, shape of the flow duration curve, and hydrograph shape.

Given the inherent errors in input and observed data and the approximate nature of model formulations, absolute criteria for watershed model acceptance or rejection are not generally considered appropriate, or widely accepted, by most modeling professionals. In contrast, most decision makers want definitive answers to the questions—"How accurate is the model?" and "Is the model good enough for this evaluation?" Consequently, the current state of the art for model evaluation is to express model results in terms of ranges that correspond to "very good," "good," "fair," or "poor" quality of simulation fit to observed behavior. These characterizations inform appropriate uses of the model: for example, where a model achieves a good to very good fit, decision-makers often have greater confidence in having the model assume a strong role in evaluating management options. Conversely, where a model achieves only a fair or poor fit, decision makers may assume a much less prominent role for the model results in the overall weight-of-evidence evaluation of management options.

For HSPF and similar watershed models, a variety of performance targets have been documented in the literature, including Donigian et al. (1984), Lumb et al. (1994), Donigian (2000), and Moriasi et al. (2007). Based on these references and past experience, the HSPF performance targets for simulation of hydrology are summarized in Table 3-1. Model performance is generally deemed fully acceptable where a performance evaluation of "good" or "very good" is attained. It is important to clarify that the tolerance ranges are intended to be applied to mean values, and that individual events or observations may show larger differences and still be acceptable (Donigian, 2000).

The model calibration generally attempts to achieve a good balance between the relative error metrics and the Nash-Sutcliffe coefficient of model fit efficiency (NSE; Nash and Sutcliffe, 1970). Unlike relative error, NSE is a measure of the ability of the model to explain the variance in the observed data. Values may vary from $-\infty$ to 1.0. A value of NSE = 1.0 indicates a perfect fit between modeled and observed data, while values equal to or less than 0 indicate the model's predictions of temporal variability in observed flows are no better than using the average of observed data. The accuracy of a model increases as the value approaches 1.0. Moriasi et al. (2007) suggest that achieving a relative error on total volume of 10 percent or better and an NSE of 0.75 or more on monthly flows constitutes a good modeling fit for watershed applications.

Table 3-1. Performance targets for the HSPF hydrologic simulation (magnitude of annual and seasonal relative mean error, and daily and monthly Nash-Sutcliffe Coefficients [NSE])

Model Component	Very Good	Good	Fair	Poor
Error in total volume	≤ 5%	5 - 10%	10 - 15%	> 15%
Error in 50% lowest flow volumes	≤ 10%	10 - 15%	15 - 25%	> 25%

Error in 10% highest flow volumes	≤ 10%	10 - 15%	15 - 25%	> 25%
Error in storm volume	≤ 10%	10 - 15%	15 - 25%	> 25%
Winter volume error (JFM)	≤ 15%	15 - 30%	30 - 50%	> 50%
Spring volume error (AMJ)	≤ 15%	15 - 30%	30 - 50%	> 50%
Summer volume error (JAS)	≤ 15%	15 - 30%	30 - 50%	> 50%
Fall volume error (OND)	≤ 15%	15 - 30%	30 - 50%	> 50%
NSE on daily values	> 0.80	> 0.70	> 0.60	≤ 0.60
NSE on monthly values	> 0.85	> 0.75	> 0.65	≤ 0.65

3.2 SNOW

Snow accumulation and melt is an important part of hydrology in this northern watershed and snow dynamics were recalibrated following the model extension. Monthly snow water equivalent (SWE) simulated by the HSPF model were compared to observed snow data available from the National Snow and Ice Data Center (NSIDC). The NSIDC SNOw Data Assimilation System (SNODAS) data products integrate remote sensing snow data from satellites, ground observations and aircrafts to provide estimates of snow cover and associated parameters (Carroll et al., 2001). SWE data are available from September 2003 to present at a spatial resolution of 1 km by 1 km and a temporal resolution of one day for the continental United States. HSPF simulated time-series were compared to SNODAS SWE to guide the calibration of snow accumulation and melt in the watershed. The calibration focus period was January 2004 through September 2021.

During the snow depth calibration process, values of parameters in the SNOW-PARM1 and SNOW-PARM2 blocks of the HSPF model were configured by land cover type or for the whole study area. The calibrated values of these parameters are provided in Table 3-2. Table 3-3 provides calibration metrics to compare observed and simulated snow water equivalent watershed-wide. Graphical comparisons for the watershed are shown in Figure 3-1. In general, the parameters are within recommended ranges and the fit to SWE data is good. The calibrated CCFACT parameter, however, which is the condensation/convection melt factor that influences snow pack melt timing, is below the recommended range. Values within the range speed the snow melt process, degrading the model fit to both observed SWE data and streamflow timing in the spring following snow melt. The minimum allowable value in HSPF is 0.0 and calibration of other HSPF watershed models have also applied lower CCFACT values to enhance the hydrologic simulation.

Table 3-2. HSPF snow calibration parameter values

Parameter	Description	Calibrated Value or Range	Recommended Range
SHADE	Fraction shaded from solar radiation, varied by land use/cover	0.1 – 0.85	0 - 0.8
SNOWCF	Snow gage catch correction factor	1.1	1.0 - 2.0
COVIND	Snowfall required to fully cover surface	0.4	0.1 - 10.0
RDCSN	Density of new snow	0.15	0.05 - 0.30
TSNOW	Temperature at which precipitation becomes snow	34.0	30.0 - 40.0
SNOEVP	Snow evaporation factor	0.1	0.0 - 0.5
CCFACT	Condensation/convection melt factor	0.2	0.5 - 8.0
MWATER	Liquid water storage capacity in snowpack	0.03	0.005 - 0.2

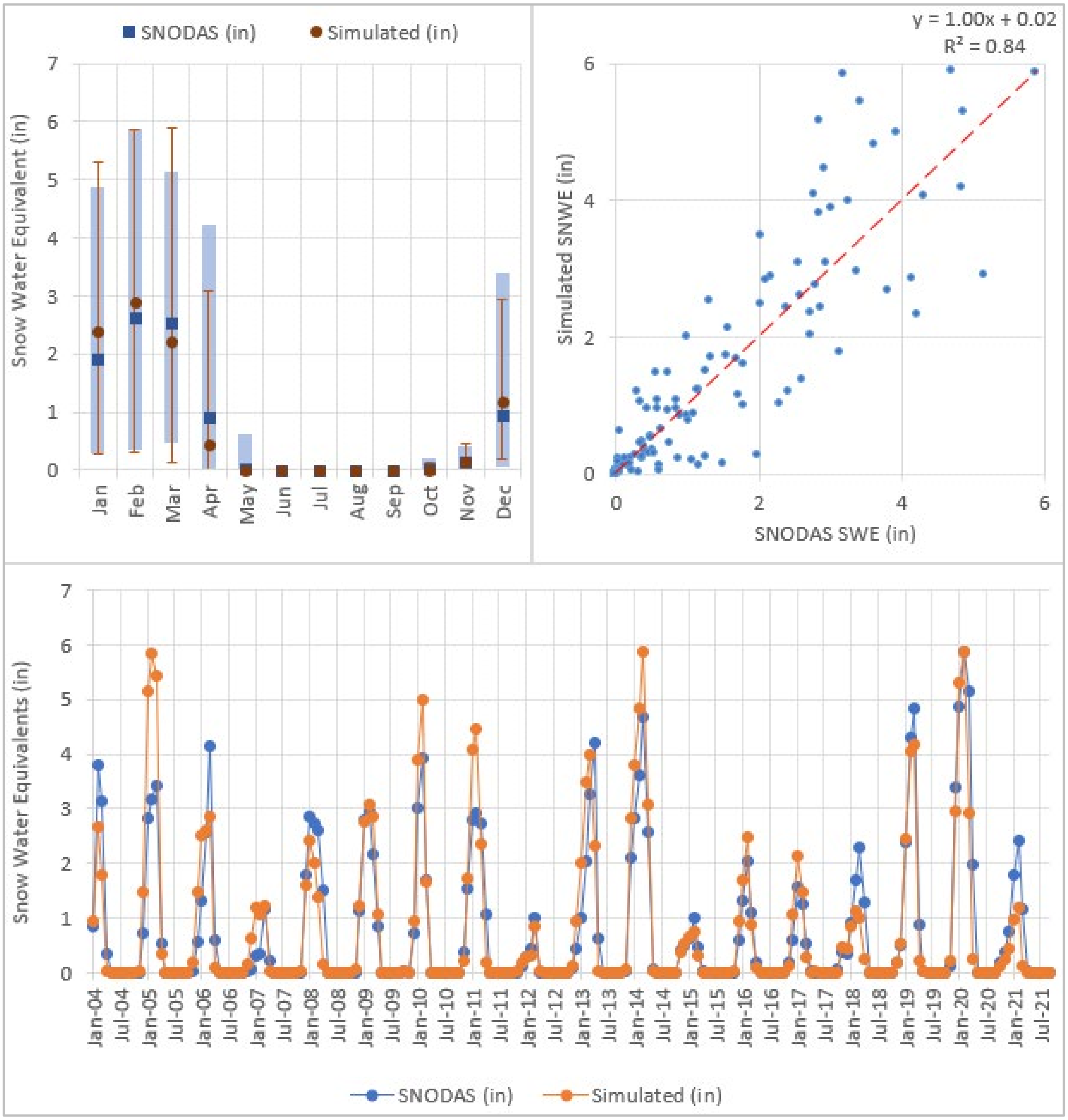

Figure 3-1. Graphical comparison of SNODAS and HSPF simulated snow water equivalent for the watershed

Table 3-3. Statistical comparison of SNODAS and HSPF simulated snow water equivalent for the watershed

Parameter	Relative error (Δsim obs)	Monthly NSE	Monthly R^2
Snow Water Equivalent	2%	0.80	0.84

3.3 EVAPOTRANSPIRATION

Evapotranspiration (ET) is the sum of transpiration of soil water by plants and evaporation of water from the soil matrix, standing/open water, and leaf surfaces (e.g., intercepted precipitation). ET is crucial to the hydrologic calibration because it is the largest component of the water balance in a watershed. Actual ET has often been unconstrained in watershed models due to a lack of observed data. However, remotely sensed, gridded ET data are now available for model applications, including the Simplified Surface Energy Balance (SSEBop) dataset that provides estimates of global terrestrial ET (Savoca et al, 2013). SSEBop uses the Simplified Surface Energy Balance (SSEB) approach (Senay et al 2007, 2011a, 2011b, 2013) to estimate actual ET as a function of remotely sensed MODIS thermal imagery (acquired every eight days). In some Minnesota HSPF simulations in the past, MODIS ET data have been used directly as a comparison to simulated ET. While both MODIS and SSEBop perform similarly well on an annual time step, it has been found that SSEBop appears to produce a less biased result than MODIS across different land uses and climate zones (Velpuri et al., 2013). Thus, SSEBop was applied for the hydrologic calibration. SSEBop ET data products are currently available for 2000 – 2021, and the portion overlapping the HSPF model simulation period was used for calibration. These data are imprecise because these are not direct measurements of actual ET, however, are useful for checking that modeled ET patterns are realistic, and the estimates are applied as such.

Monthly ET estimates for the watershed were extracted from the global SSEBop dataset. The gridded data were aggregated for the watershed to support the ET calibration. The aggregated monthly data were compared to ET (TAET) simulated by the model and used to inform parameterization. The pattern of observed monthly evapotranspiration was also used to refine the precipitation interception (MON-INTERCEP) and lower soil zone ET (MON-LZETPARM) parameter blocks in the HSPF model.

Figure 3-2 shows mean monthly simulated evapotranspiration in comparison with SSEBop estimates for the watershed. Summary statistics are listed in Table 3-4. Overall, the model closely matches SSEBop estimates of ET, both in terms of magnitude and seasonal pattern.

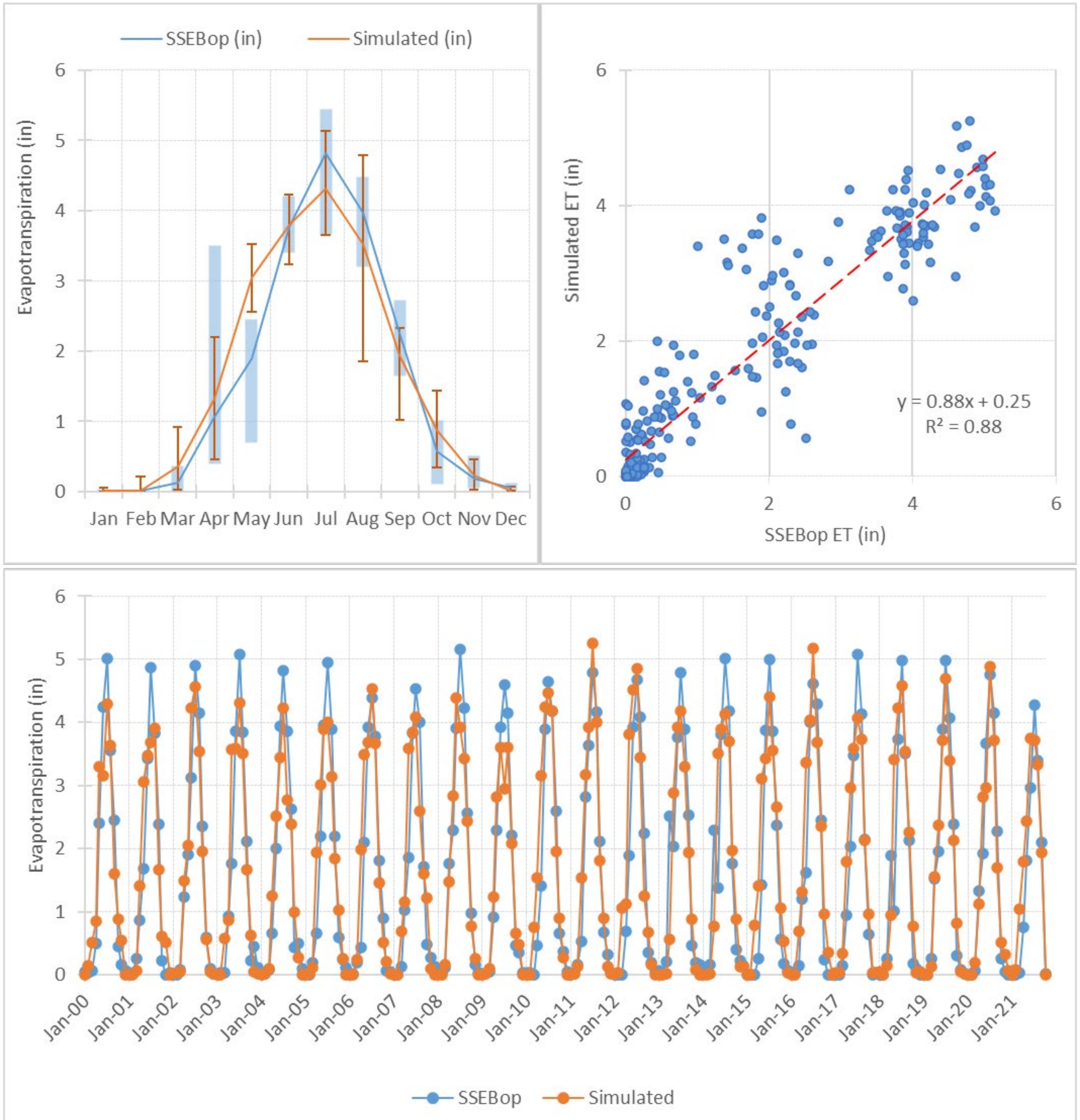

Figure 3-2. Graphical comparison of SSEBop ET and HSPF simulated ET for the watershed

Table 3-4. Statistical comparison of SSEBop ET and HSPF simulated ET for the watershed

Parameter	Relative error (Δsim obs)	Monthly NSE	Monthly R^2
ET	4%	0.88	0.88

3.4 WATER BALANCE

The overall water balance estimated by the model for the study area is summarized in Figure 3-3. The major component of outflow is ET, although the fraction of supply going to ET is somewhat lower than would be expected for this ecoregion (Sanford and Selnick, 2013), reflecting the large amount of urban impervious cover in the watershed, which promotes direct surface runoff. Approximately 58 percent of precipitation is returned to the atmosphere through evapotranspiration, while approximately 42 percent becomes streamflow.

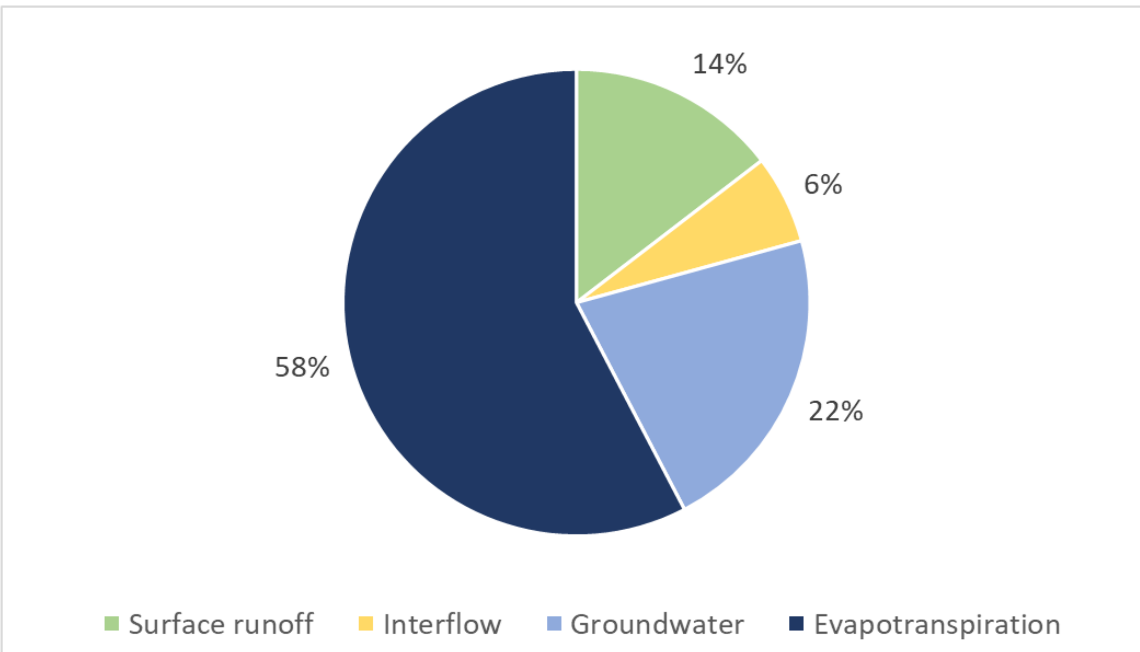

Figure 3-3. Pervious land water balance

3.5 STREAMFLOW CALIBRATION AND VALIDATION

The flow calibration was completed by comparing time-series model results to gaged daily average flow. Key considerations in the hydrology calibration included total flow, the high-flow to low-flow distribution, storm flows, seasonal variations, and daily/monthly NSEs. The criteria in Table 3-1 were used to evaluate the quality of model fit. Parameter values from the previous Duluth HSPF model were applied initially for the recalibration. These starting values were then modified during calibration to optimize model fit while remaining within ranges recommended by USEPA (2000) and AQUA TERRA (2012). Key hydrology parameters adjusted during calibration were USZN (upper zone soil storage), BASETP (ET from riparian vegetation), and AGWETP (ET from shallow groundwater). Final parameter values are contained in the accompanying model user control input (.uci) file.

The hydrologic simulation was tuned using gaging records between Water Year (WY) 2012 and WY 2021. Sites with longer periods of record were primarily used for calibration, whereas sites with shorter periods of record were used for validation purposes. Several of the available flow gages have very brief periods of record, do not operate in winter (due to ice), and the seasonal start often occurs during spring snowmelt, so complete water balances cannot be calculated. The hydrologic response of a stream to weather events incorporates persistence because of antecedent soil moisture and groundwater stores, and statistics for short periods of record can easily be distorted by an imprecise estimation of the volume of one or two storm events. For watershed model calibration we prefer to use continuous gage records of 10 years in length to average out the impacts of these temporal distortions and specify a separate period for model validation. Such data are not available Duluth streams.

Results of the hydrologic calibration are summarized in Table 3-5. In many cases, the model appears to under-predict flow volumes. Nonetheless, the error in total flow volume fit is rated as “good” or “very good” for four of the nine sites and as “fair” for Mission Creek and Miller Creek. The total volume fit is “poor” for Lester River, East Branch Amity Creek, and Keene Creek. For Lester River there is no wintertime monitoring, and it appears the model may be representing snowmelt too early, resulting in much of the snowmelt volume being discharged before springtime monitoring begins. This is especially evident in April 2013 where monthly simulated flow is 50 percent less than monthly observed flow. Statistics for East Branch Amity Creek are affected by the apparent simulated misrepresentation of baseflow recession in summer 2012; however, the observed baseflow recession does not appear to be explained by the precipitation record. Statistics for Keene Creek are affected by the apparent underestimation of a few large storm peaks in the summer of 2015; however, these reported peaks do not appear to be fully explained by the precipitation record.

The error in 10 percent highest flows fit is rated as “good” or “very good” for five of the nine sites and as “fair” for Amity Creek, Lester River, and Tischer Creek. The 10 percent highest flows fit is “poor” for East Branch Amity Creek. Simulated flow in April 2013 for Amity Creek, Lester River, and East Branch Amity Creek are all 50 percent low compared to observed and this misrepresented snowmelt, or rain on snow, event pulls down the overall 10 percent highest flows statistical result into the “fair” and “poor” range. On the other hand, Tischer Creek has monitoring in March 2016 where simulated flow is approximately 25 percent greater than observed and this misrepresented snowmelt, or rain on snow, event pushes up the overall 10 percent highest flows statistical result into the “fair” range.

The fit for flows below the median (i.e., 50th percentile) is ranked as “poor” at six stations, “fair” at one, and only ranked as “good” and “very good” for Merritt Creek and East Branch Amity Creek sites. Baseflows for many of these urban streams are less than 2 cfs, which could lead to larger uncertainty bounds in the gage record; however, it is also possible that there are unaccounted for sources of flow, ranging from lawn irrigation to regional groundwater discharge. Large percent errors on small flows can be misleading and are often small in terms of total magnitude as is the case here.

For Amity Creek, a log timeseries plot of simulated and observed streamflow (Figure 3-4) shows that the simulation captures observed trends and magnitudes but occasionally underestimates the lowest of low flows. A monthly box and whisker plot (Figure 3-5) shows the simulation generally capturing monthly median, 10th percentile, and 90th percentile streamflows. A flow duration curve (Figure 3-6) and daily scatter plot (Figure 3-7) show good agreement throughout the flow regime and an unbiased scatter around a line of equal fit. For Mission Creek, a log timeseries plot of simulated and observed streamflow (Figure 3-8) shows that the simulation generally captures observed trends and magnitudes as does (Figure 3-9) that shows the monthly median, 10th percentile, and 90th percentile streamflows. A flow duration curve (Figure 3-10) and daily scatter plot (Figure 3-11) show the simulation is biased high from the 30th to 85th percentile and biased low above the 90th percentile and an unbiased scatter around a line of equal fit.

When and where the model is rated fair to poor based on model fit statistics is in part due to anthropogenic and natural uncertainties or unknowns as well as due to the length and timing of the gage records. Many of the other components of the water balance appear to be well constrained, including precipitation (Section 2.1), snow depth

(Section 3.2), and soil moisture and evapotranspiration (Section 3.3). In addition, it appeared that adjacent gages (such as Lester River and Amity Creek) required different sets of parameters to achieve optimal fit, so the final parameter set represents a compromise across the full study area. It is believed that the most reliable flow gages are the MNDNR/HYDSTRA gages with long records (i.e., Amity Creek, Lester River, and Mission Creek), and greater weight should be placed on results from those stations when evaluating the model as a whole. At these stations flow model fits are similar to or better than the previous Duluth model.

Table 3-5. Summary statistics for hydrologic calibration and validation

Station	Location	HSPF Reach	Error in Total Volume	Error in 50% Low Flows	Error in 10% High Flows	Daily NSE	Monthly NSE
Calibration (WY 2012 to WY 2021); sites with longer periods of record							
HYDSTRA 02038001	Amity Creek at Duluth	436 + 438	-9.2%	31.7%	-20.3%	0.786	0.810
HYDSTRA 02036003	Lester River near Duluth	499	-18.0%	-18.2%	-23.5%	0.733	0.764
HYDSTRA 03010003	Mission Creek near Fond du Lac	201	11.4%	62.1%	-3.3%	0.775	0.752
Validation (WY 2012 to WY 2021); sites with shorter periods of record							
HYDSTRA 02040008	Chester Creek at W. College Street	386	-5.8%	27.0%	-8.8%	0.694	0.776
HYDSTRA 02037005	East Branch Amity Creek at Duluth, 1.8 miles downstream of CSAH37	454	-29.4%	10.6%	-33.3%	0.684	0.583
HYDSTRA 03189016	Keene Creek at Duluth	302	-18.3%	-26.4%	-17.8%	0.639	0.601
HYDSTRA 03163011	Merritt Creek at Duluth	321	-7.0%	7.0%	-10.0%	0.645	0.388
HYDSTRA 03163011	Miller Creek at Duluth	330	-13.3%	-37.6%	-8.2%	0.539	0.645
HYDSTRA 02039008	Tischer Creek at Duluth	409 + 412	3.2%	-29.4%	20.6%	0.298	0.743

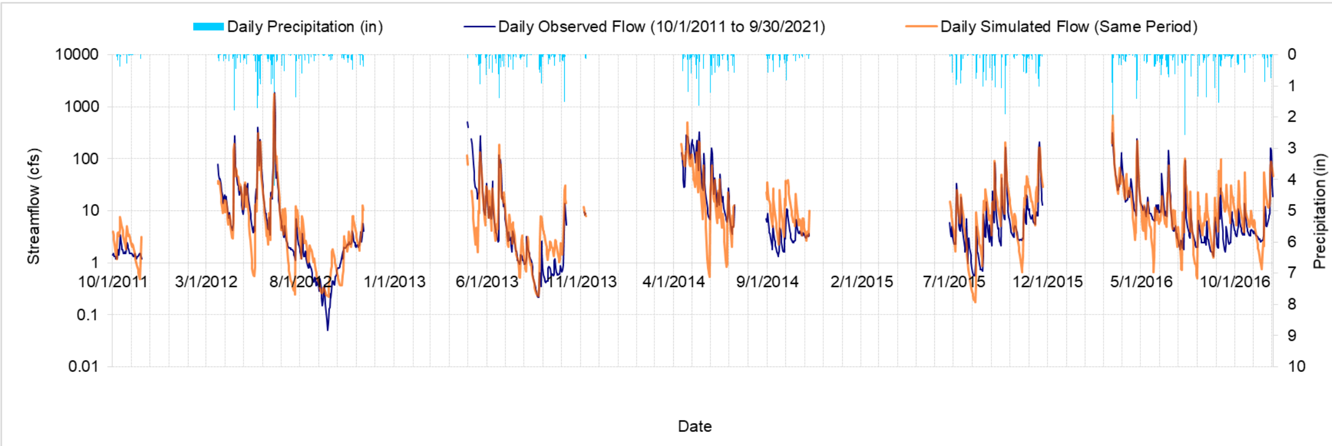

Figure 3-4. Time series of observed and simulated streamflow at Amity Creek at Duluth

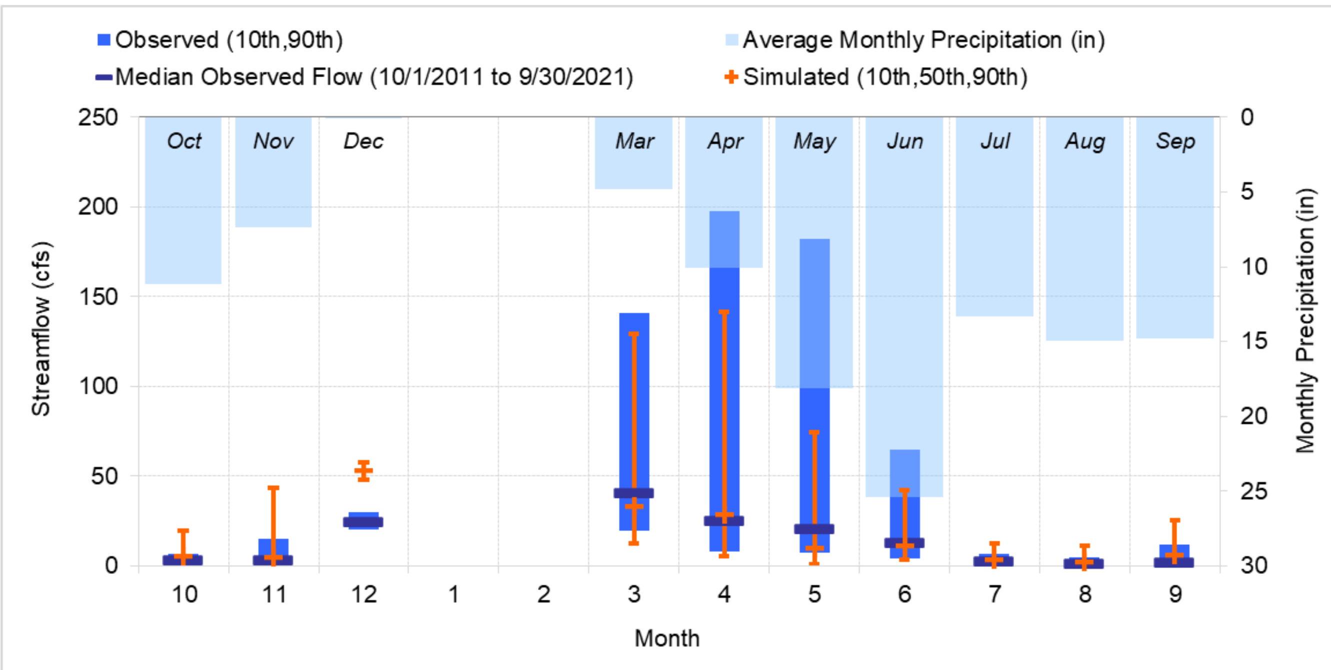

Figure 3-5. Observed and simulated 10th, 50th, and 90th percentile monthly flows for Amity Creek at Duluth

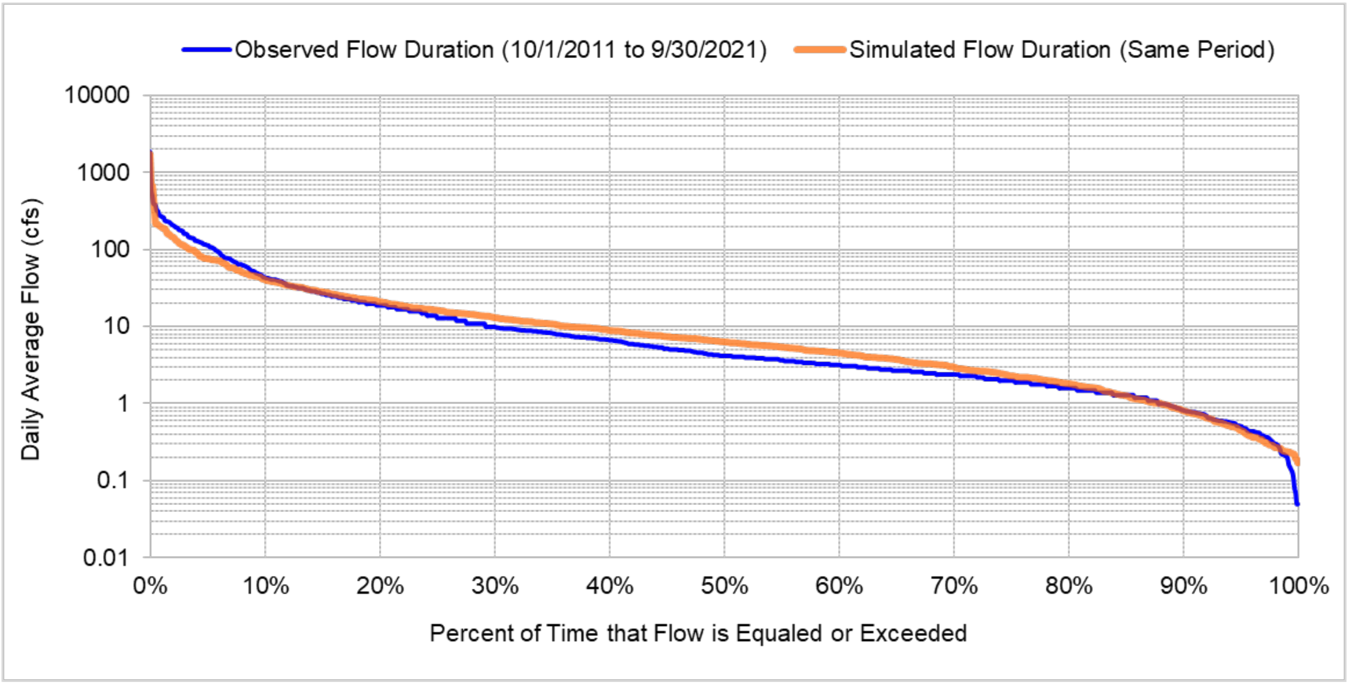

Figure 3-6. Observed and simulated flow duration curves for Amity Creek at Duluth

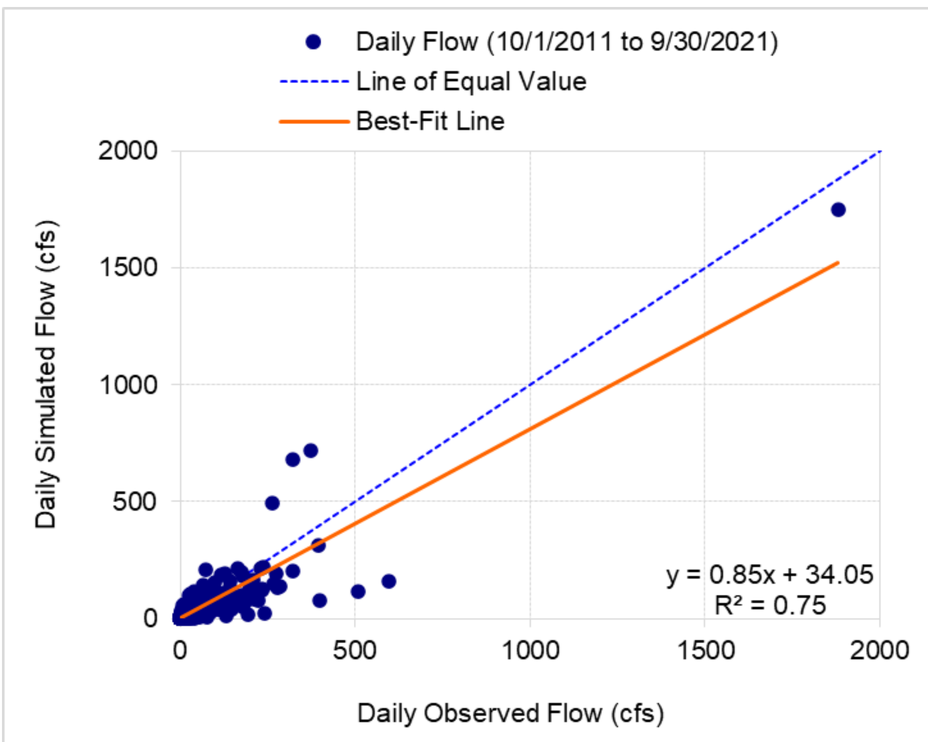

Figure 3-7. Scatterplot of observed and simulated daily flows for Amity Creek at Duluth

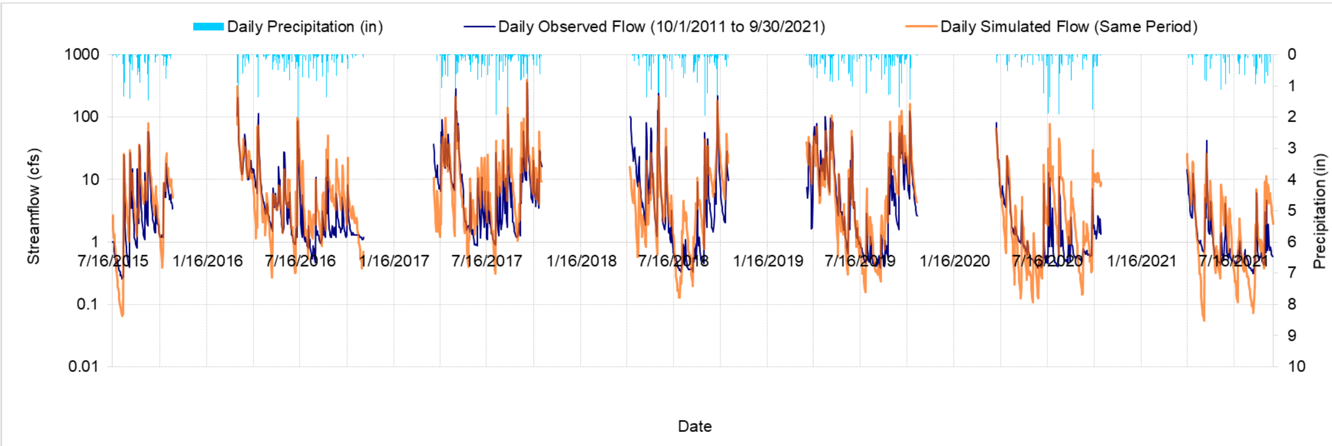

Figure 3-8. Time series of observed and simulated streamflow at Mission Creek near Fond du Lac

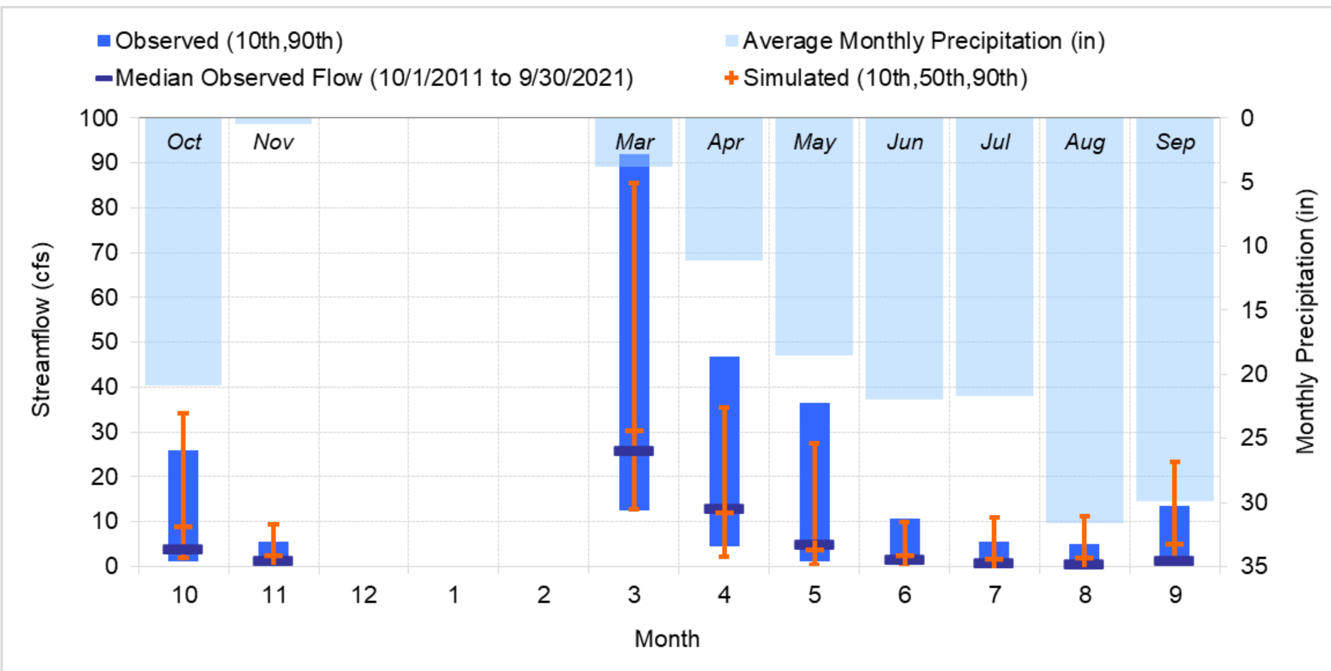

Figure 3-9. Observed and simulated 10th, 50th, and 90th percentile monthly flows for Mission Creek near Fond du Lac

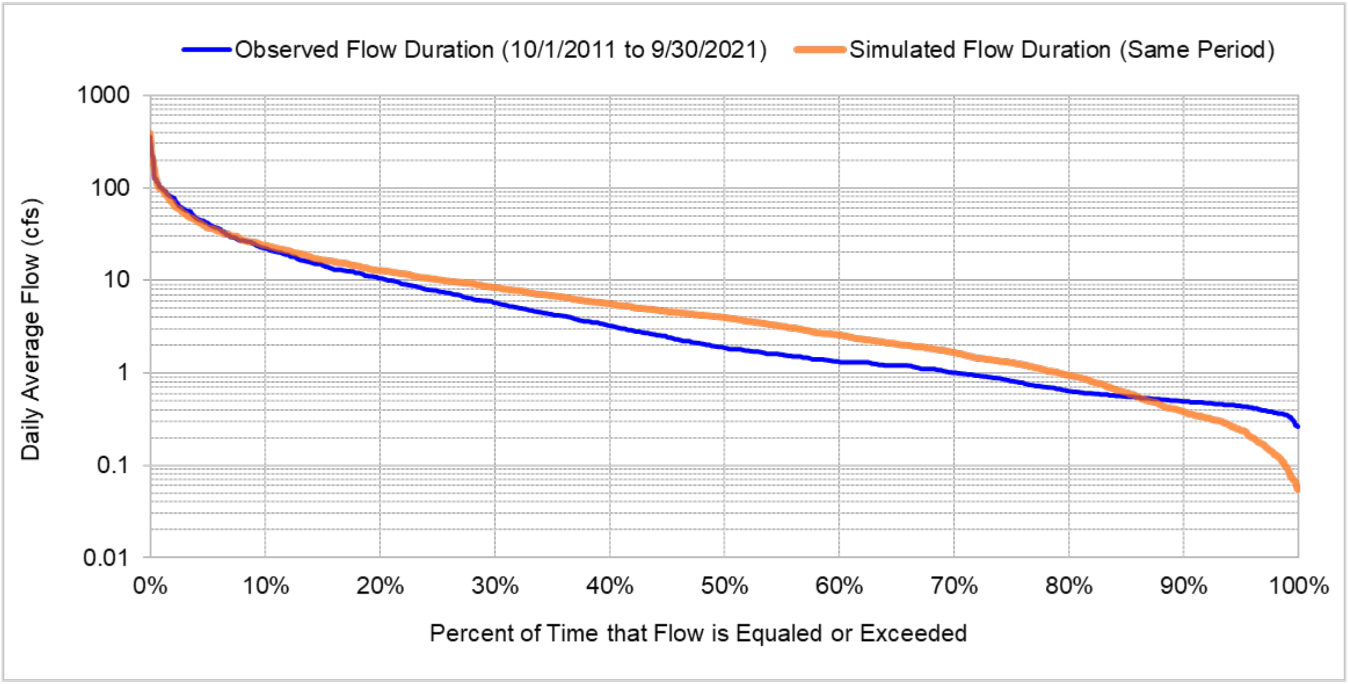

Figure 3-10. Observed and simulated flow duration curves for Mission Creek near Fond du Lac

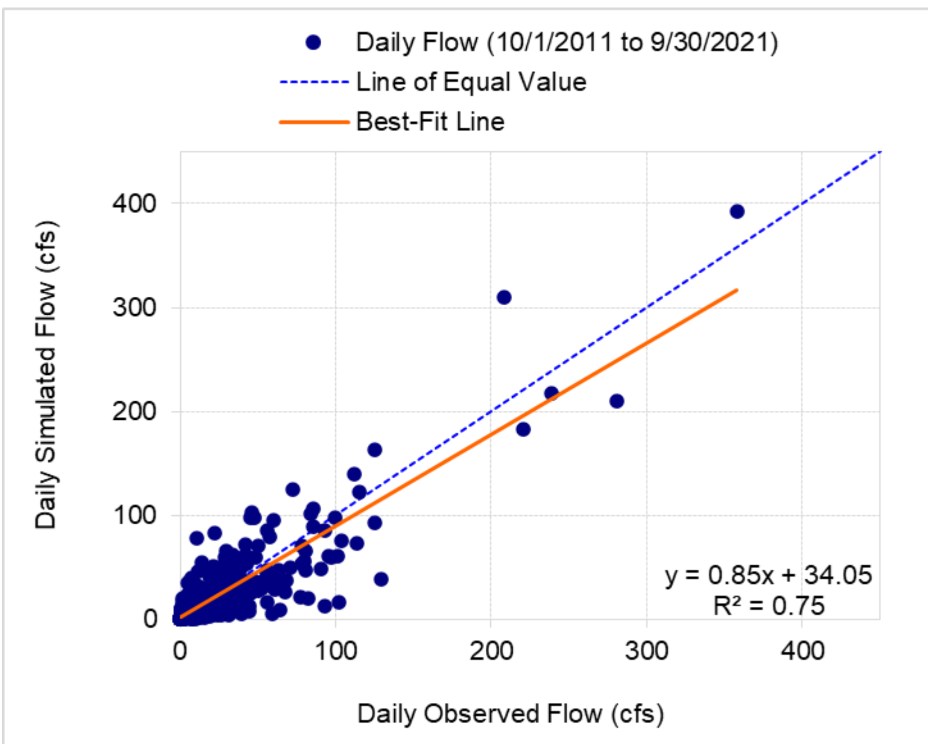

Figure 3-11. Scatterplot of observed and simulated monthly flows for Mission Creek near Fond du Lac

4.0 SEDIMENT CALIBRATION AND VALIDATION

4.1 APPROACH

Important aspects of sediment behavior within a watershed system include loading and erosion sources, delivery of these eroded sediment sources to streams, drains and other pathways, and subsequent instream transport, scour and deposition processes (USEPA, 2006). Sediment calibration for watershed models involves numerous steps in estimating model parameters and determining appropriate adjustments needed to insure a reasonable simulation of the sediment sources on the watershed, delivery to the waterbody, and transport behavior within the channel system. Rarely is there observed local data at sufficient spatial detail to obtain a unique calibration for all parameters for all land uses and each stream and waterbody reach. Consequently, modelers focus the calibration efforts on sites with observed data and review simulations in all parts of the watershed to ensure that the model results are consistent with field observations, historical reports, and expected behavior from experience (Donigian and Love, 2003, AQUA TERRA, 2012).

Sediment calibration for the Duluth urban area was undertaken in accordance with AQUA TERRA (2012) as well as the guidelines in USEPA (2006). The sediment calibration entails multiple elements. Upland sediment yields were refined to align with reference and field data. The instream simulation was also tuned; this involved analyzing the shear stress simulation in the reaches and setting scour and deposition thresholds to expected typical values. The long-term behavior of sediment in the channels was constrained to ensure that degradation or aggradation amounts were physically realistic and consistent with available local information. The sediment calibration also compared and calibrated instream modeled sediment to stream monitoring records. Throughout this process the relative contribution of upland versus channel-derived sediment was evaluated and adjustments were made to achieve a reasonable balance that aligns with information available.

HSPF simulates sediment yield to streams in two stages. First, HSPF calculates the detachment rate of sediment by rainfall (in tons/acre/hour) as

$$DET = (1 - COVER) \cdot \mathrm{SMPF} \cdot KRER \cdot P^{JRER}$$

where *DET* is the detachment rate (tons/acre/hour), *COVER* is the dimensionless factor accounting for the effects of cover on the detachment of soil particles, *SMPF* is the dimensionless management practice factor, *KRER* is the coefficient in the soil detachment equation, *JRER* is the exponent in the soil detachment equation, and *P* is precipitation depth in inches over the simulation time interval. Direct addition of detached sediment (e.g., from wind deposition to the land surface) can also be added via the parameter *NVSI*. Actual detached sediment storage available for transport (*DETS*) is a function of accumulation over time and the reincorporation rate, *AFFIX*.

The transport capacity for detached sediment from the land surface (*STCAP*) is represented as a function of overland flow:

$$STCAP = KSER\ (SURS + SURO)^{JSER}$$

where *KSER* is the coefficient for transport of detached sediment, *SURS* is surface water storage (inches), *SURO* is surface outflow of water (in/hr), and *JSER* is the exponent for transport of detached sediment.

DET is similar in concept to the Universal Soil Loss Equation (USLE; Wischmeier and Smith, 1978), which predicts sediment detachment as a function of is the rainfall erosivity, *RE*, a soil erodibility factor, *K*, a length-slope factor, *LS*, a cover factor, C*,* and a practice factor, *P*:

$$DET = RE \cdot K \cdot LS \cdot C \cdot P.$$

KRER was estimated as the soil erodibility coefficient provided by SSURGO, gap filled with STATSGO. The primary upland calibration parameter for sediment is *KSER*, which determines the ability of overland flow to transport detached sediment. HSPF can also simulate gully erosion in which sediment generated from the land surface is not constrained by rainfall detachment.

The key parameters controlling channel erosion, deposition, and sediment transport within streams and rivers are as follows (USEPA, 2006):

KSAND: Sand transport is represented with a power function based on average velocity, such that carrying capacity for sand = *KSAND* x $AVVEL^{EXPSND}$. *KSAND* was adjusted to improve the comparison between simulated and observed suspended sediment concentrations and to ensure a reasonable evolution of sand storage over time.

TAUCD: HSPF calculates bed shear stress (*TAU*) during each model time step for each individual reach. The critical bed shear stress for deposition (lb/ft^2) represents the energy level below which cohesive sediment (silt and clay) begins to deposit to the bed. Initial values of *TAUCD* for silt and clay were estimated by reach by examining the cumulative distribution function of simulated shear stress and setting the parameter to a lower percentile of the distribution in each reach segment, as recommended by USEPA (2006). This was done after the recalibration of hydrology. The 20th percentile was used for clay and the 25th percentile for silt initially for free-flowing streams, and then these were adjusted regionally, and on a reach-by-reach basis during the sediment calibration.

TAUCS: The critical bed shear stress for scour (lb/ft^2) represents the energy level above which scour of cohesive sediment begins. Initial values of *TAUCS* were set, as recommended, at upper percentiles of the distribution of simulated shear stress in each reach (the 90th percentile for clay and the 95th percentile for silt for free-flowing streams). These were adjusted regionally, and on a reach-by-reach basis during the sediment calibration.

M: The erodibility coefficient of the sediment (lb/ft^2-d) determines the maximum rate at which scour of cohesive sediment occurs when shear stress exceeds *TAUCS*. This coefficient is a calibration parameter. It was initially set to values obtained during the original model calibration. These were adjusted regionally, and on a reach-by-reach basis during the calibration.

Calibration for sediment and other water quality parameters differs from calibration for hydrology in that pollutant concentrations are in most cases not continuously monitored. Instead, observations typically provide measurements of conditions at a point in time and point in space via a grab sample. The discrete nature of these samples presents problems for model calibration: A sample that represents a point in time could have been obtained from a system where conditions are changing rapidly over time – for instance, the rising limb of a storm hydrograph. Such samples cannot be expected to be matched by a model prediction of a daily average concentration. On the other hand, there may be large discrepancies between dynamic model predictions of hourly concentrations and data that are a result of small timing errors in the prediction of storm event flow peaks. Spatially, grab samples reflect conditions in one part of a stream reach (which may or may not be composited over the width and depth of a cross section). HSPF model results, in contrast, represent average concentrations over the length of a stream reach which is assumed to be fully mixed. Model predictions and field observations inevitably have some degree of mismatch in space and time and, even in the best models, will not fully match. Accordingly, a statistical best fit approach is needed to guide the calibration and rate the performance.

Performance targets for sediment calibration, based on Donigian (2000) and Duda et al. (2012), are summarized in Table 4-1. These performance targets are evaluated for both concentration and load, where load is estimated from concentration on paired data, and should only be applied in cases where there is a minimum of 20 observations. Model performance is generally deemed acceptable where a performance evaluation of "good" or "very good" is attained.

Table 4-1. Performance targets for HSPF sediment simulation (magnitude of annual and seasonal relative error on daily values)

Model Component	Very Good	Good	Fair	Poor
Suspended Sediment	≤ 20%	20 - 30%	30 - 45%	> 45%

4.2 SEDIMENT SOURCES

4.2.1 Upland Sheet, Rill and Gully Erosion

Sediment calibration for watershed models involves numerous steps in estimating model parameters and determining appropriate adjustments needed to insure a reasonable simulation of the sediment sources on the watershed, delivery to the waterbody, and transport behavior within the channel system. When performing sediment calibration in HSPF for the Duluth urban area, we followed the process discussed in AQUA TERRA (2012) as well as USEPA (2006). While there are many steps in the process, the overarching goal is to achieve an appropriate balance between upland and near-channel sources. Upland sediment loading rates vary widely from place to place and are influenced by local conditions such as soil erodibility, slope, and precipitation patterns. Land use also has a strong influence on sediment yield, and most studies show the lowest rates from forest and other uses with good vegetation cover, somewhat higher rates for relatively unmanaged grasslands, high rates for developed land and pasture/hay production, and the highest rates for cropland. Loading rates from urban land can be elevated by the effects of flow concentration from impervious surfaces, higher runoff volumes, and erosion hotspots in ditches and ephemeral headwater channels receiving flow from storm drains. Figure 4-1 presents the average annual calibrated unit area loads for each land use/cover category in the Duluth area model. Some model land uses classes, like residential, are made up of both pervious and impervious surfaces. Relative rankings and magnitudes of unit area loading are similar to the previous Duluth model.

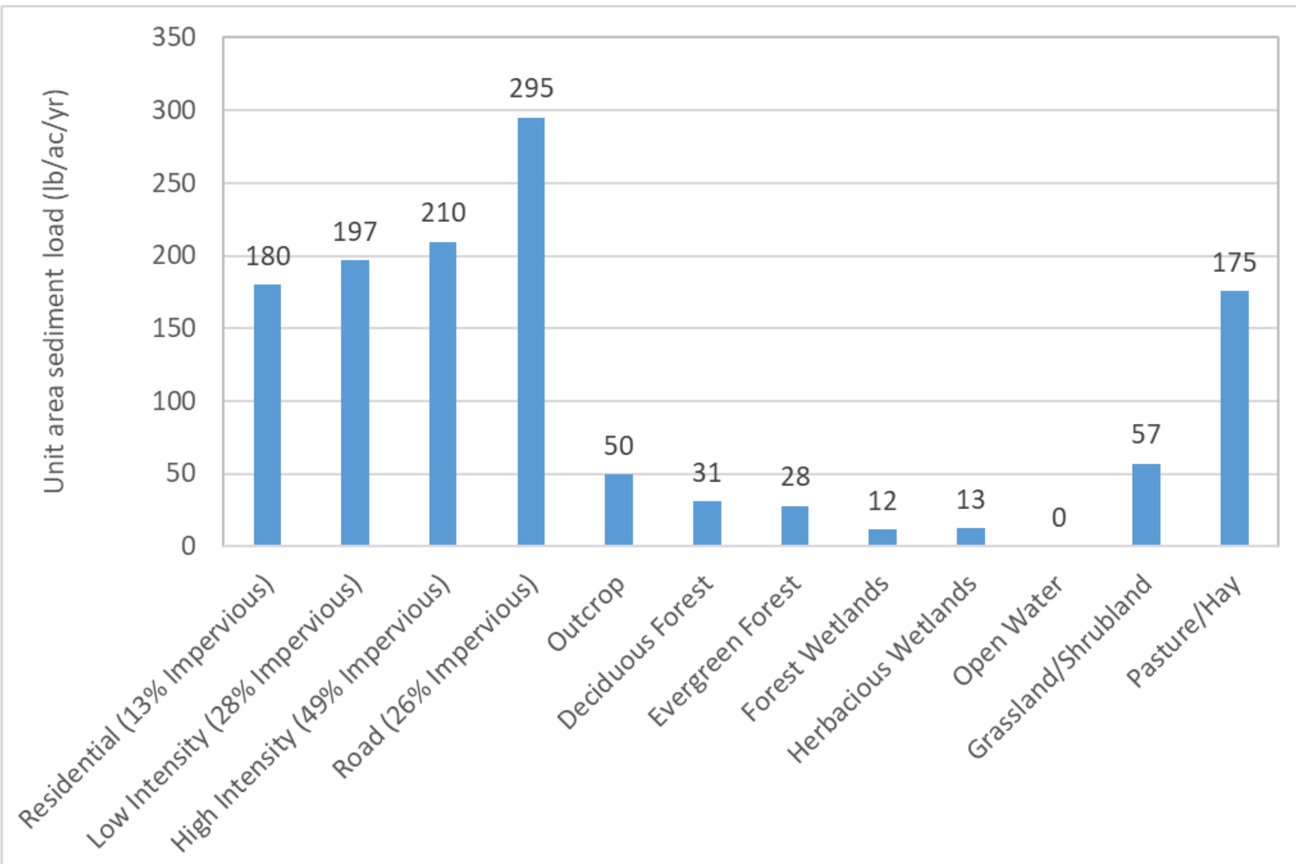

Figure 4-1. Annual average upland sediment yields for the Duluth urban area HSPF model

4.2.2 Reach Sediment Dynamics

Net sediment scour and deposition was analyzed on a reach-by-reach basis consistent with recommendations in USEPA (2006) to ensure that significant amounts of scour and deposition occur only in areas where reasonably expected (e.g., accumulation of sediment in reservoirs). Because HSPF is a one-dimensional reach model, the simulated change in bed depth encompasses changes in channel width (i.e., bank erosion) as well as bed depth. Stream power during large storm events can suspended bed sediment and transport it downstream, and powerful flows may also reshape the channel, removing sediment from the streambanks. During lower flow periods suspended sediment settles, contributing to bed and bank storages. Sediment settles more readily through the water column of slow moving or stagnant waters, depositing and accumulating in the bed. Change in simulated stream bed depth for reaches in the model is shown in the figures that follow. The average change across the reaches is -0.07 ft for the length of multi-decade simulation. Net changes in reach sediment of this magnitude are quite reasonable. Additional information on the geomorphic classes can be found in the previous report (Tetra Tech, 2019).

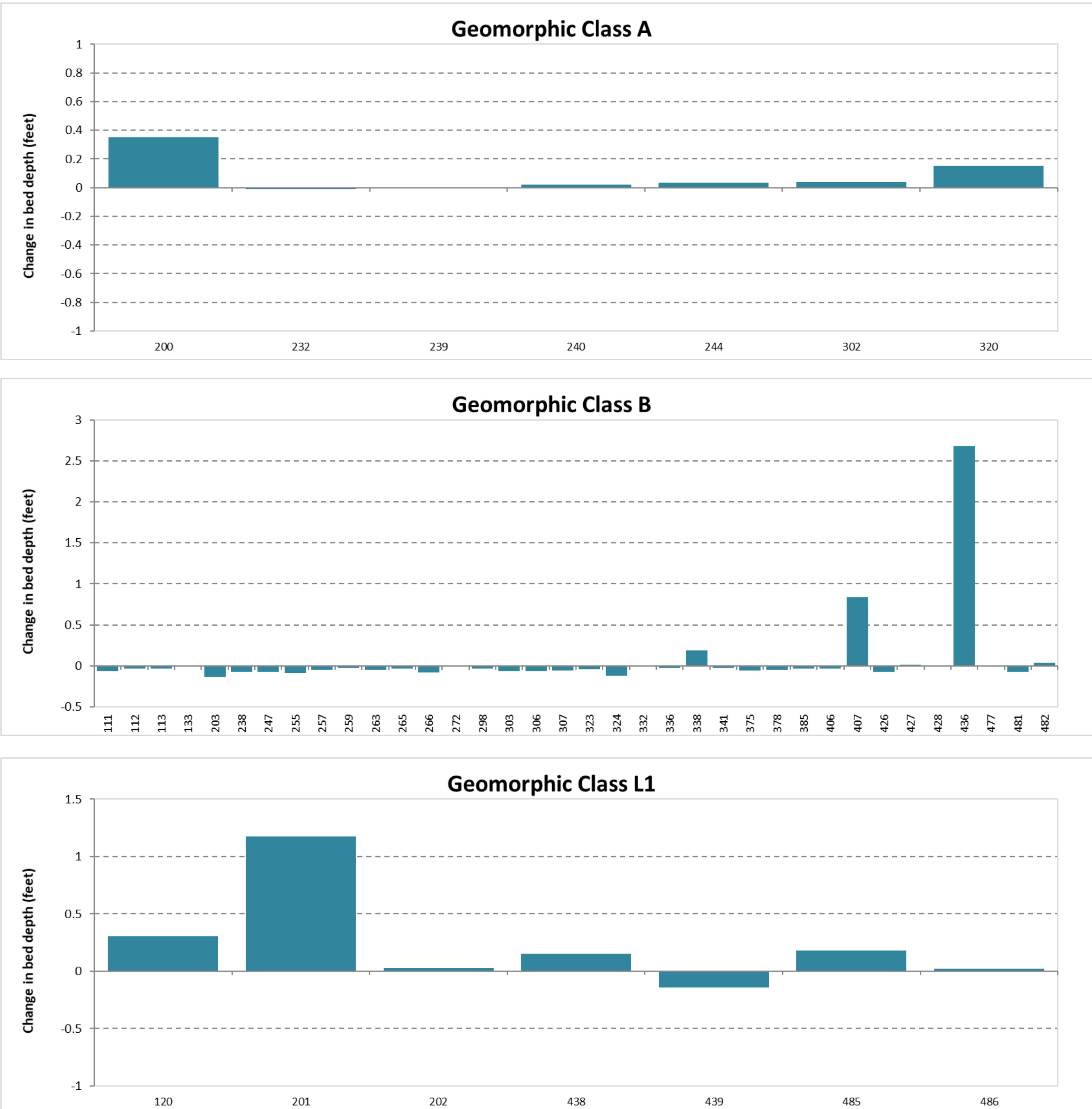

Figure 4-2. Net change in bed depth (ft) for HSPF model reaches by geomorphic class (A, B, and L1)

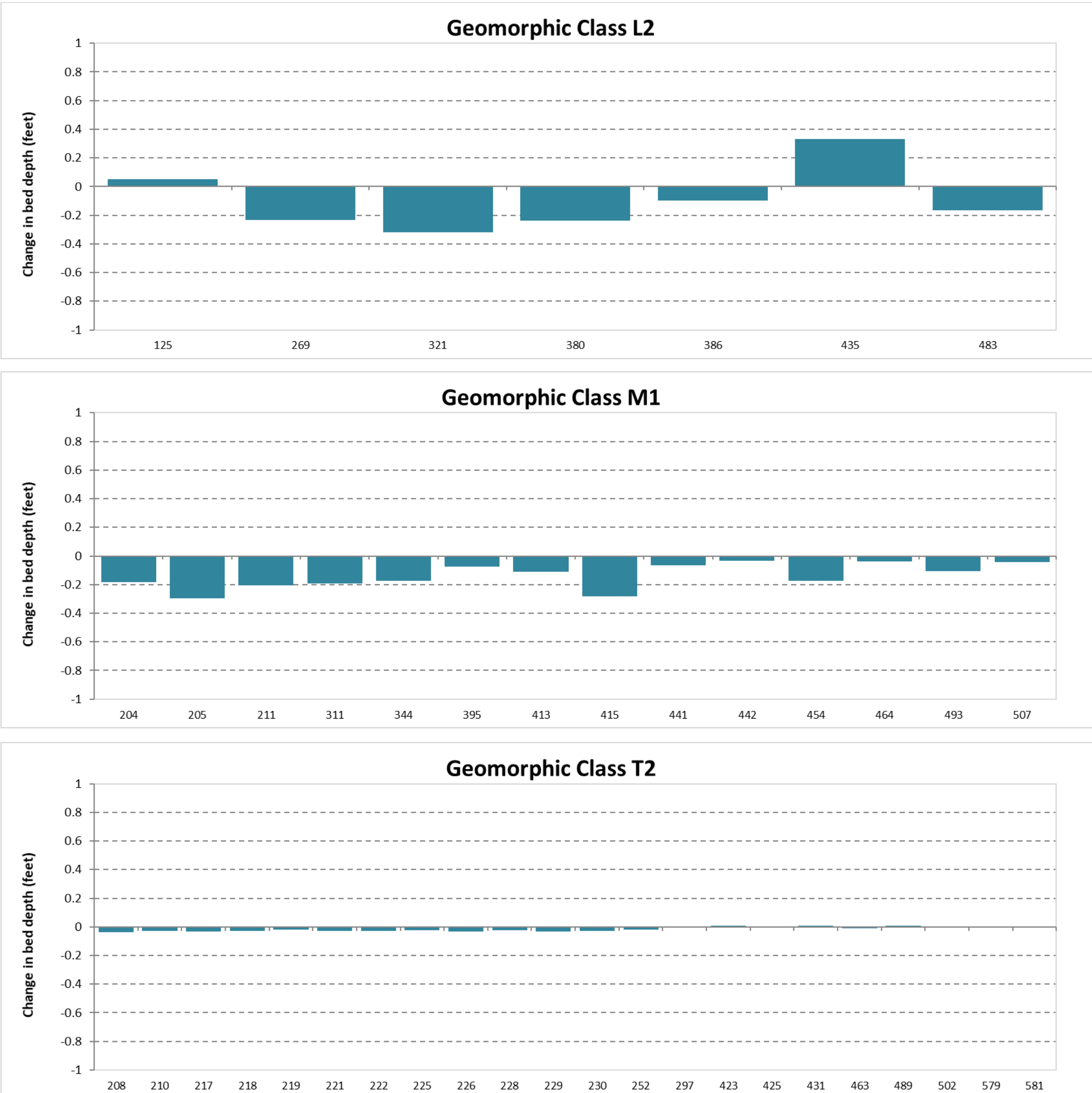

Figure 4-3. Net change in bed depth (ft) for HSPF model reaches by geomorphic class (L2, M1, and T2)

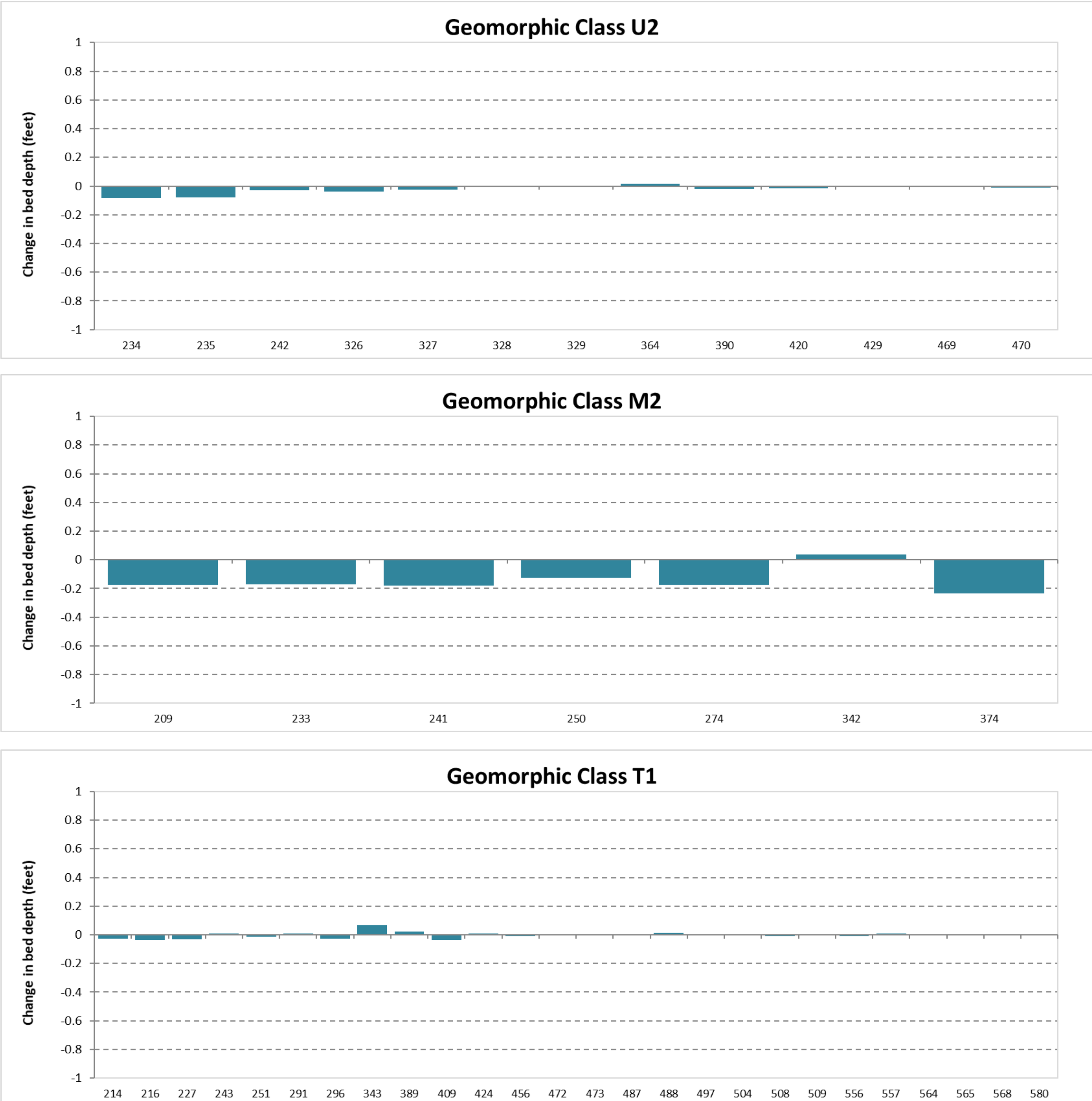

Figure 4-4. Net change in bed depth (ft) for HSPF model reaches by geomorphic class (U2, M2, & T1)

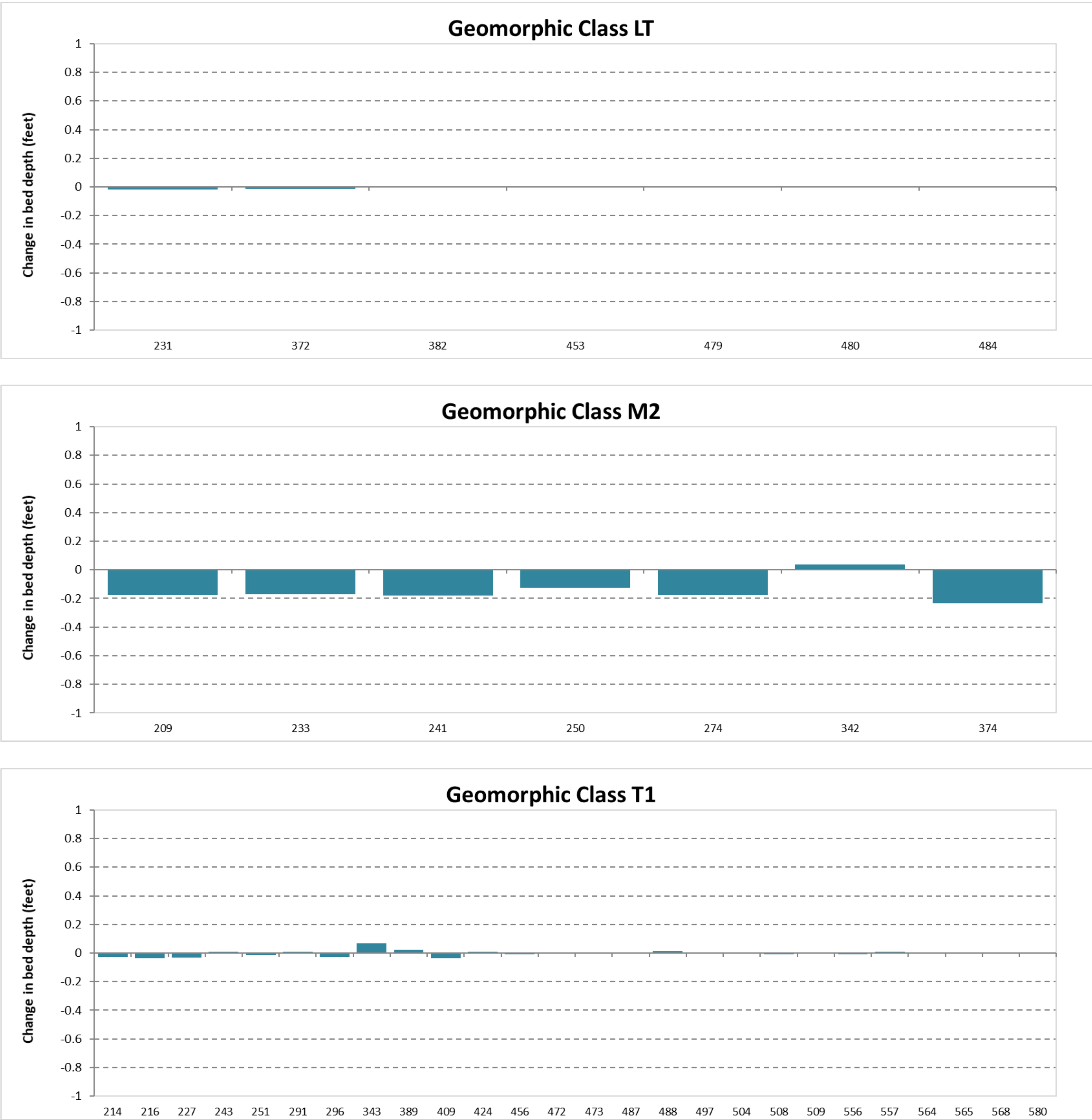

Figure 4-5. Net change in bed depth (ft) for HSPF model reaches by geomorphic class (LT, M2, T1)

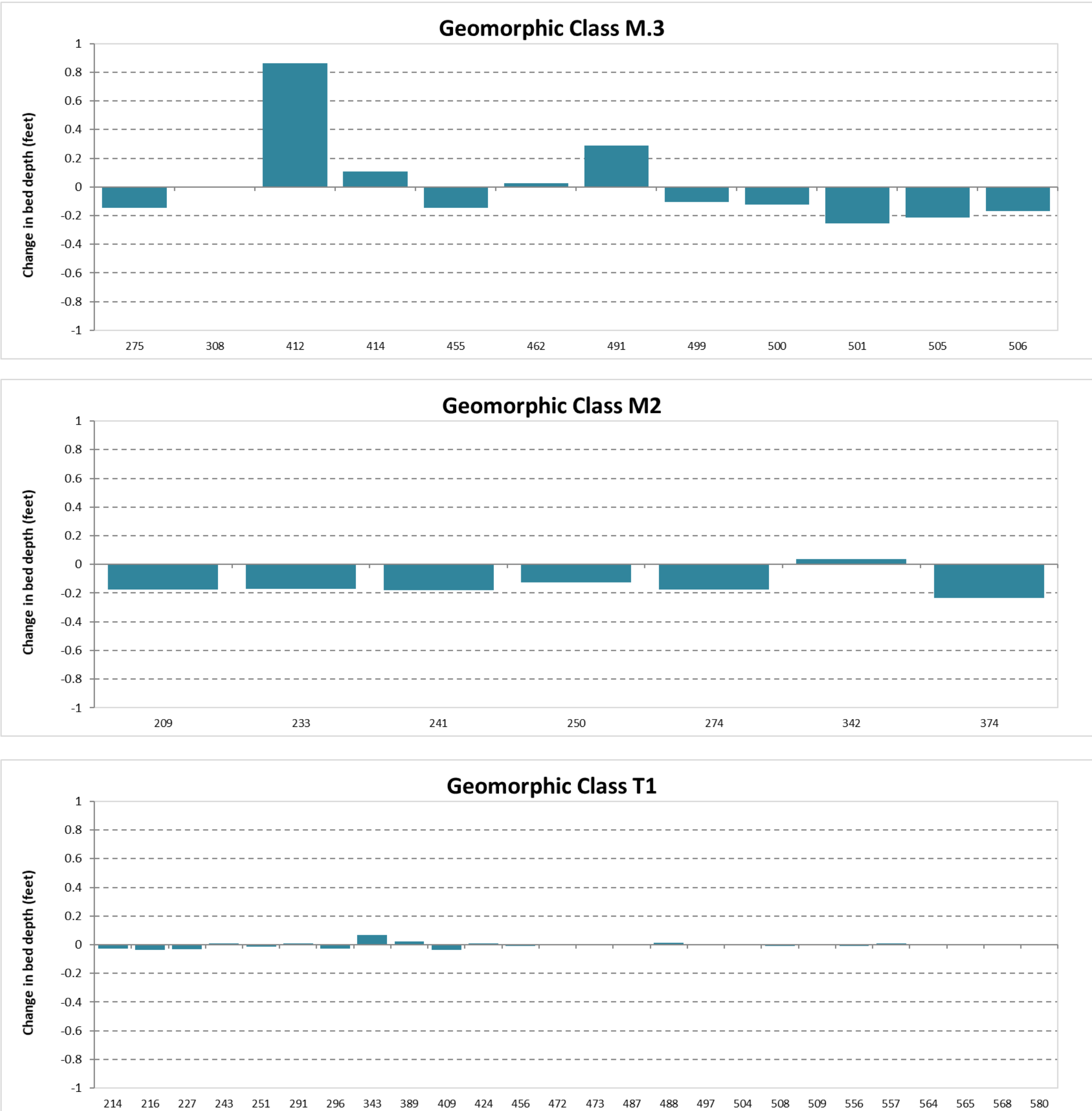

Figure 4-6. Net change in bed depth (ft) for HSPF model reaches by geomorphic class (M.3, M2, T1)

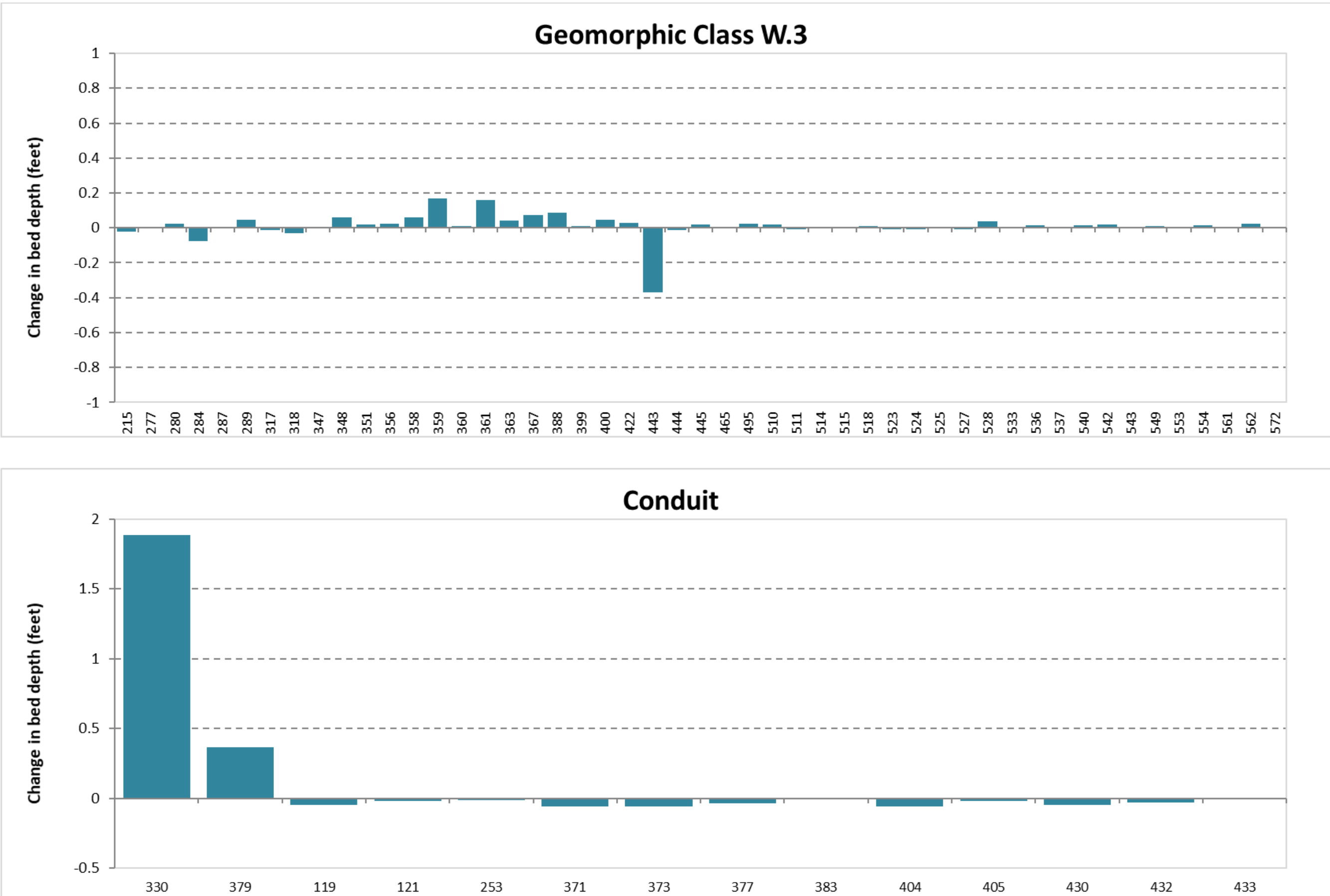

Figure 4-7. Net change in bed depth (ft) for HSPF model reaches by geomorphic class (W.3 and conduit)

4.2.3 Sediment Source Apportionment

Sediment source contributions simulated by the model are shown in Figure 4-8. Sediment sources include near-channel sources (i.e., the net scouring and deposition of the sediment bed and bank) and upland sediment sources (i.e., sheet and rill erosion).

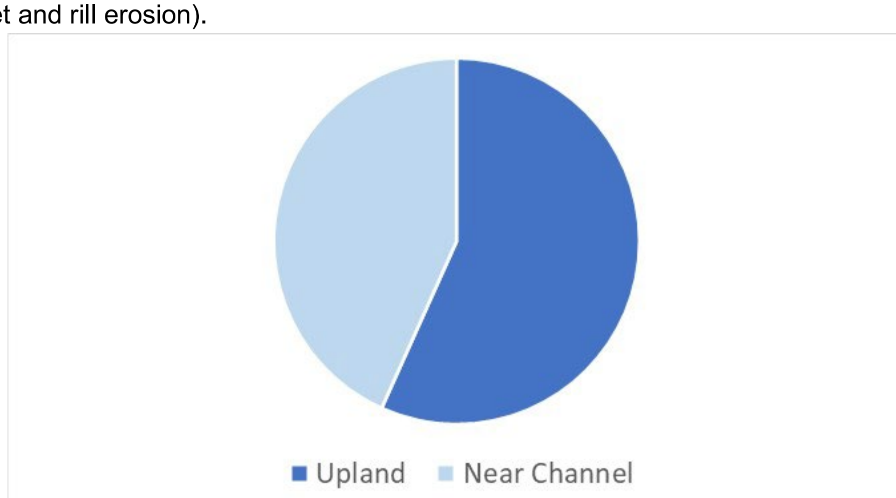

Figure 4-8. Sources of sediment simulated by the HSPF model

4.3 CALIBRATION AND VALIDATION TO OBSERVED SUSPENDED SOILIDS

Suspended sediment calibration took place at multiple stations in the watershed and used both visual and statistical approaches. The calibration effort attempted to replicate the observed time series while at the same time minimizing relative errors associated with both concentration and load (as inferred from concentration and flow). Attention was paid to matching observed and simulated relationships between concentration and flow using power plots, while also examining the distribution of error terms relative to both season and flow. It is not uncommon for relative average error to be strongly leveraged by one or more outliers (especially for load, which tends to be determined by concentrations at high flows); therefore, the median error, which is not sensitive to outliers, is reported as well as the average error.

Sediment calibration and validation statistics are provided in Table 4-2. For the calibration period (WY 2015 to WY 2021), five are ranked as “good” or “very good”, and one is ranked as “poor” for median relative error on concentration. For median relative error on load, all six are ranked as “very good”. For average relative error on concentration, one is ranked as “very good”, three are ranked as “fair”, and two are ranked as “poor. For average relative error on load, one is ranked as “very good”, one is ranked as “fair”, and four are ranked as “poor. The difference between “good” or “very good” rankings for medians versus “fair” and “poor” rankings for average indicate that there were one or more station specific outliers which the model did not predict. Tischer Creek has a “poor” ranking for average and median relative errors on concentration and average relative error on load, but it is rated as “very good” for median relative error on load. These results are strongly influenced by the model consistently over predicting instream sediment concentration in the summer of 2016 at this station. Overall, the sediment calibration is considered acceptable because median relative error on concentration and load are generally in the “very good” category.

For the validation period (WY 2009 to WY 2014), all stations are ranked as “very good” for median relative error on concentration and median relative error on load. For average relative error on concentration, three sites are ranked as “very good”, two are ranked as “fair”, and one is ranked as “poor”; note that average concentration is more highly influenced by outliers compared to median concentration. For average relative error on load, three are ranked as “very good”, two are ranked as “fair”, and one is ranked as “poor”. In generally, the validation period shows better results than the calibration period.

Table 4-2. TSS summary for the Duluth urban model

Station	Location	HSPF Reach	Average Observed Concentration (mg/L)	Relative Error on Concentration		Relative Error on Load	
				Ave.	Median	Ave.	Median
Calibration (WY 2015 to WY 2021)							
S001-757	Amity Creek	436 + 438	46	-26%	-3.7%	3.3%	-1.3%
S001-530, S004-953, S008-481, S007-180	Chester Creek	386	15	50%	23%	79%	8.5%
S008-482	Keene Creek	302	37	-21%	1.9%	38%	1.5%
S008-483	Merritt Creek	321	22	30%	19%	69%	8.1%

S003-071, S008-484	Miller Creek	330	24	8.7%	4.3%	37%	0.9%
S004-364, S002-480, S007-592	Tischer Creek	409 + 412	22	78%	46%	113%	15%
Validation (WY 2009 to WY 2014)							
S001-757	Amity Creek	436 + 438	92	-48%	-1.8%	-37%	0.0%
S001-530, S004-953, S008-481, S007-180	Chester Creek	386	11	21%	-1.7%	12.6%	0.0%
S008-482	Keene Creek	302	5.5	22%	-7.2%	67%	-0.3%
S004-952	Kingsbury Creek	272	49	-18%	1.7%	16.4%	0.2%
S008-483	Merritt Creek	321	8.3	-9.6%	15%	11%	3.9%
S004-364, S002-480, S007-592	Tischer Creek	409 + 412	24	9.9%	-3.5%	34%	0.0%

Example calibration plots are provided for Miller Creek and Amity Creek in Figure 4-9 to Figure 4-14. For Miller Creek, the model appears to track the observed data well, although a couple of observations above 100 mg/L are under-estimated (Figure 4-9). A log-log power plot (Figure 4-10) shows that the observed and simulated loads have a similar distribution relative to flow but are biased low in flows below 10 cfs. Lastly, the distribution of prediction errors versus flow (Figure 4-11) shows no bias relative to flow but does show the high positive error associated with the simulation overestimating the highest of observations. For Amity Creek, the model appears to track the observed data well, although a few observations above 100 mg/L are also underestimated (Figure 4-12). A log-log power plot (Figure 4-13) shows that the observed and simulated loads have a similar but biased low distribution relative to flow. Lastly, the distribution of prediction errors versus flow (Figure 4-14) shows no bias relative to flow but does show the high negative error associated with the simulation underestimating the highest of observations.

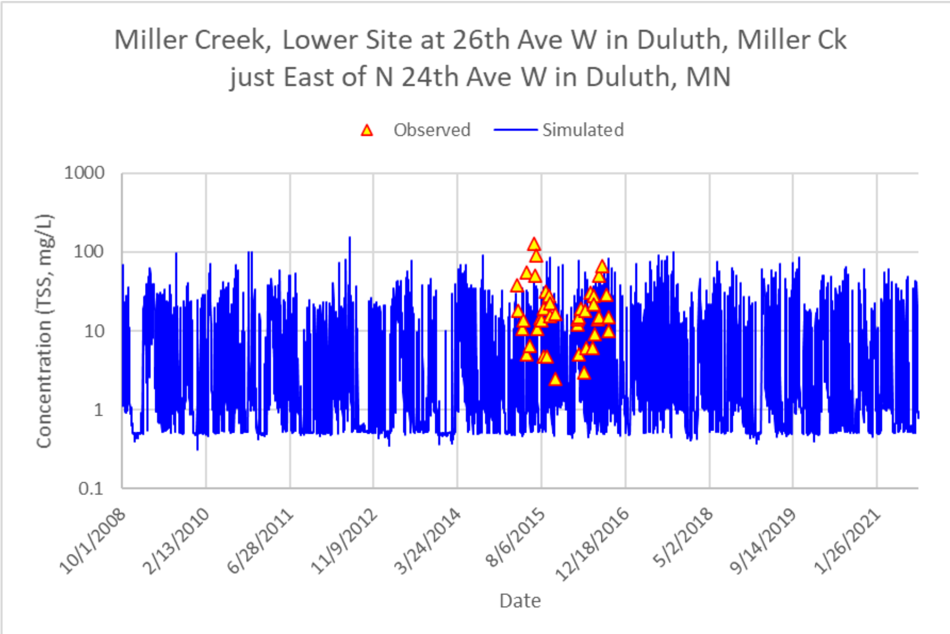

Figure 4-9. Time Series Plot for Total Suspended Sediment, Miller Creek

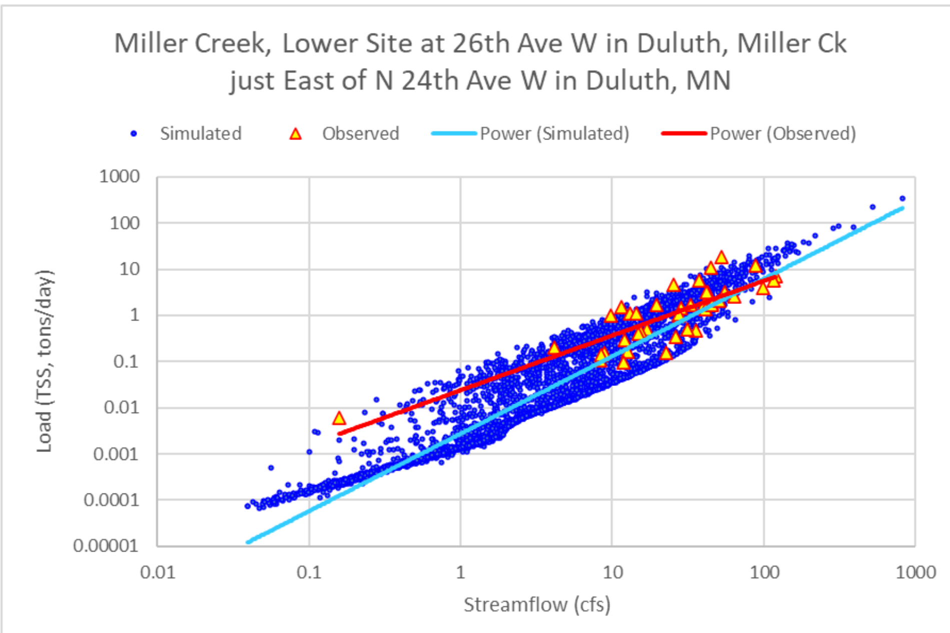

Figure 4-10. Log-log Power Plot of Simulated Total Suspended Sediment Load and Load Inferred from Observed Concentration, Miller Creek

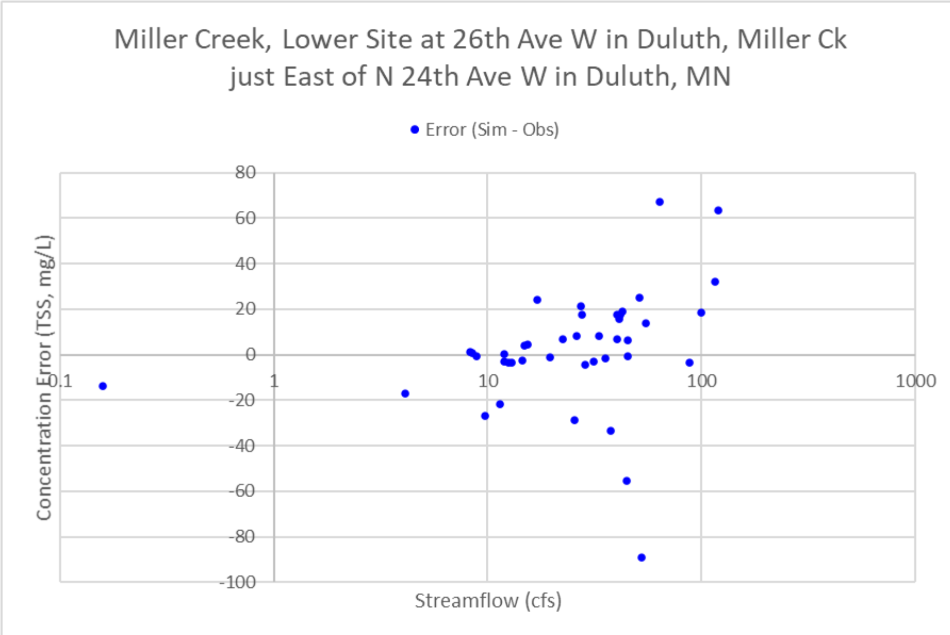

Figure 4-11. Distribution of Concentration Error for Total Suspended Sediment, Miller Creek

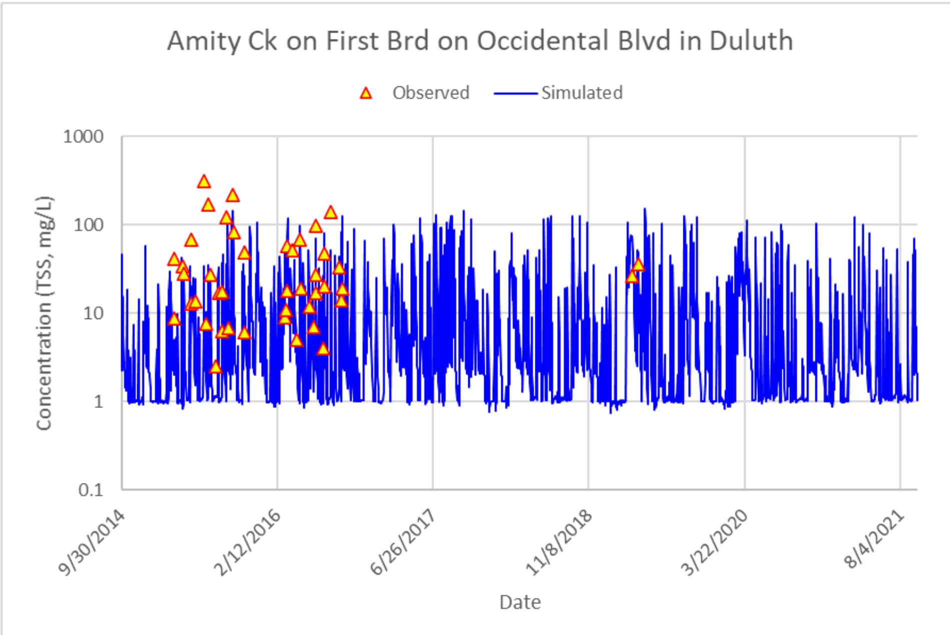

Figure 4-12. Time Series Plot for Total Suspended Sediment, Amity Creek

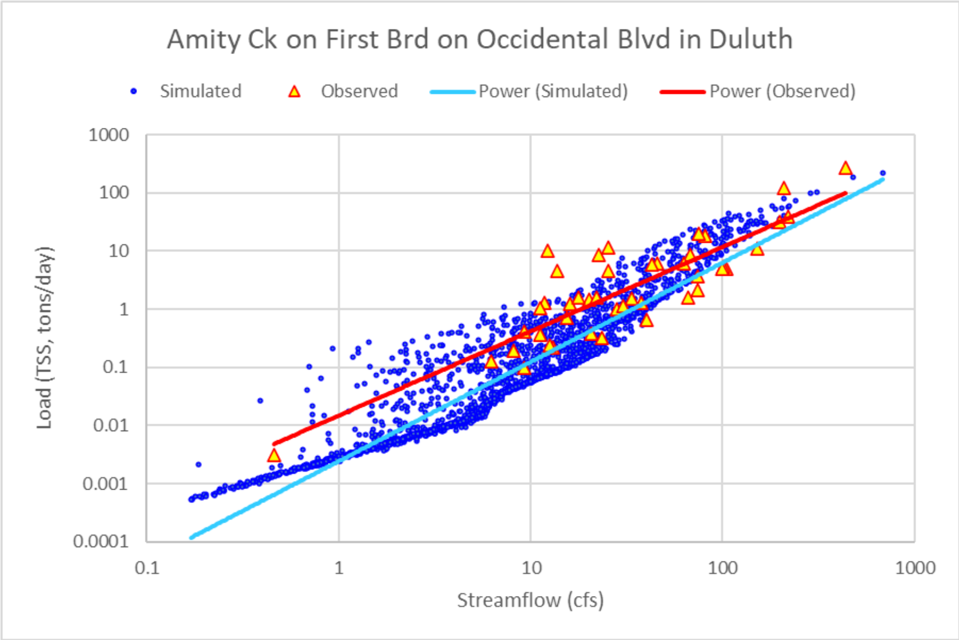

Figure 4-13. Log-log Power Plot of Simulated Total Suspended Sediment Load and Load Inferred from Observed Concentration, Amity Creek

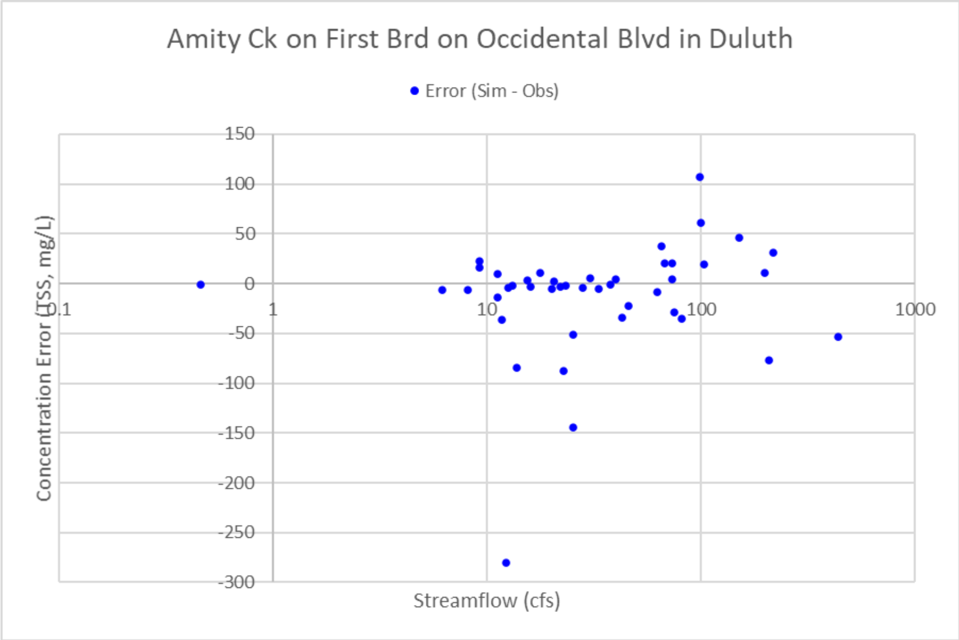

Figure 4-14. Distribution of Concentration Error for Total Suspended Sediment, Amity Creek

5.0 WATER QUALITY CALIBRATION

5.1 APPROACH

The representation of water quality and associated processes on the landscape and in streams largely depends on the simulation of hydrology and sediment transport, and the recalibration of those components is discussed in previous sections. This section presents and discusses the calibration of nutrients and organic carbon.

The HSPF model represents four nutrient constituents on the land surface as general quality constituents (GQUALs): ammonia, nitrate + nitrite, inorganic phosphorus (total orthophosphate), and organic matter. Each of these constituents is then partitioned into alternative species at the point-of-entry to the reach network:

- Inorganic nitrogen is partitioned into dissolved nitrate, dissolved ammonium, and sorbed ammonium. Fractions of the dissolved constituents are set to reproduce observed data, while sorption of ammonium is simulated using equilibrium partitioning assumptions (the model connects ammonia from the land surface to dissolved N in the stream reach, but equilibrium partitioning to the sorbed form occurs instantaneously). Partitioning of ammonium between dissolved and sorbed forms depends on local suspended sediment concentrations.
- Inorganic phosphorus is partitioned into dissolved and sorbed fractions using equilibrium partitioning assumptions. As with ammonium, the fraction that becomes sorbed depends on the local suspended sediment concentration.
- Organic matter (biomass) is partitioned into labile and refractory organic carbon, organic nitrogen, and organic phosphorus components.

All four upland components (ammonia, nitrate + nitrite, inorganic phosphorus, and organic matter) may be loaded through either surface flow or subsurface flow (interflow discharge and resurfacing shallow groundwater). The HSPF GQUAL algorithms do not maintain a full mass balance of subsurface constituents (which would require linkage to a groundwater quality model); rather, the user specifies concentration values, which may vary monthly, for interflow and groundwater for each constituent. Surface loading is considered from both pervious and impervious surfaces.

For most water quality constituents, it is unreasonable to propose that the model predict all temporal variations in concentration and load. The model should, however, provide an accurate representation of long-term and seasonal trends in concentration and load for important constituents, and correctly represent the relationship between flow and load. To ensure this, it is important to use statistical tests of equivalence between observed and simulated concentrations, rather than relying on a pre-specified model tolerance on difference in concentrations.

Ideally, average errors and average absolute errors should both be low, reflecting a lack of bias and high degree of precision, respectively. In many cases, the average error statistics will be inflated by a few highly discrepant outliers. It is therefore also useful to compare the median error statistics, which are less influenced by outlier values.

General performance targets for water quality simulation with HSPF are provided by Duda et al. (2012) and are shown in Table 5-1. These are calculated from observed and simulated daily concentrations and should only be applied in cases where there is a minimum of 20 observations to reduce impact of anomalous outliers.

Table 5-1. Performance targets for HSPF water quality simulations (magnitude of annual and seasonal relative average error (RE))

Model Component	Very Good	Good	Fair	Poor
Water quality/nutrients	≤ 15%	15 - 25%	25 - 35%	> 35%

Evaluation of water quality simulations presents many challenges because, unlike flow, water quality is generally not monitored continuously. Grab samples at a point in space and time may not be representative of average conditions in a model reach on a given day due to either spatial or temporal uncertainty (i.e., an instantaneous measurement in time may deviate from the daily average, especially during storm events, while a point in space may not be representative of average conditions across an entire model reach). Where constituent concentrations are near reporting levels, relative uncertainty in reported results is naturally high. Accurate information on daily variability in point source loads is also rarely available, particularly for minor facilities.

5.2 NUTRIENTS

5.2.1 Upland Calibration

Mean annual simulated TN and TP unit area loading rates are provided for the HSPF model in Figure 5-1 and Figure 5-2; these were calibrated using reference ranges from the literature as discussed in Tetra Tech (2019) and according to instream nutrient grab sample records collected in Duluth area streams. Calibrated unit area loading rates are comparable to rates in the literature. For example, simulated annual average nitrogen loading rates for urban land uses (e.g., developed, low) range from about 2.0 to 6.5 lb/ac/yr, which is within the reference range for developed land (i.e., 2 – 17 lb/ac/yr; Tetra Tech, 2019). Similarly, simulated annual average phosphorus loading rates for urban land uses range from 0.26 to 0.41 lb/ac/yr (literature range for developed land is 0.17 – 1.5 lb/ac/yr as discussed in Tetra Tech, 2019).

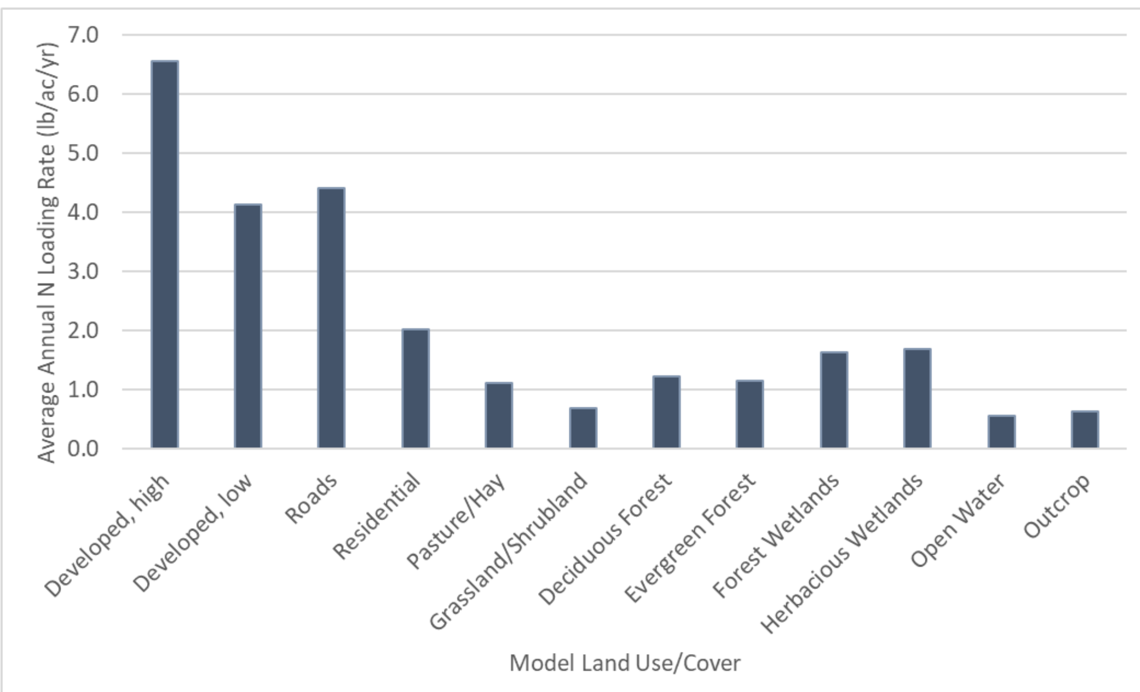

Figure 5-1. Annual average upland TN loading rates by model land use/cover

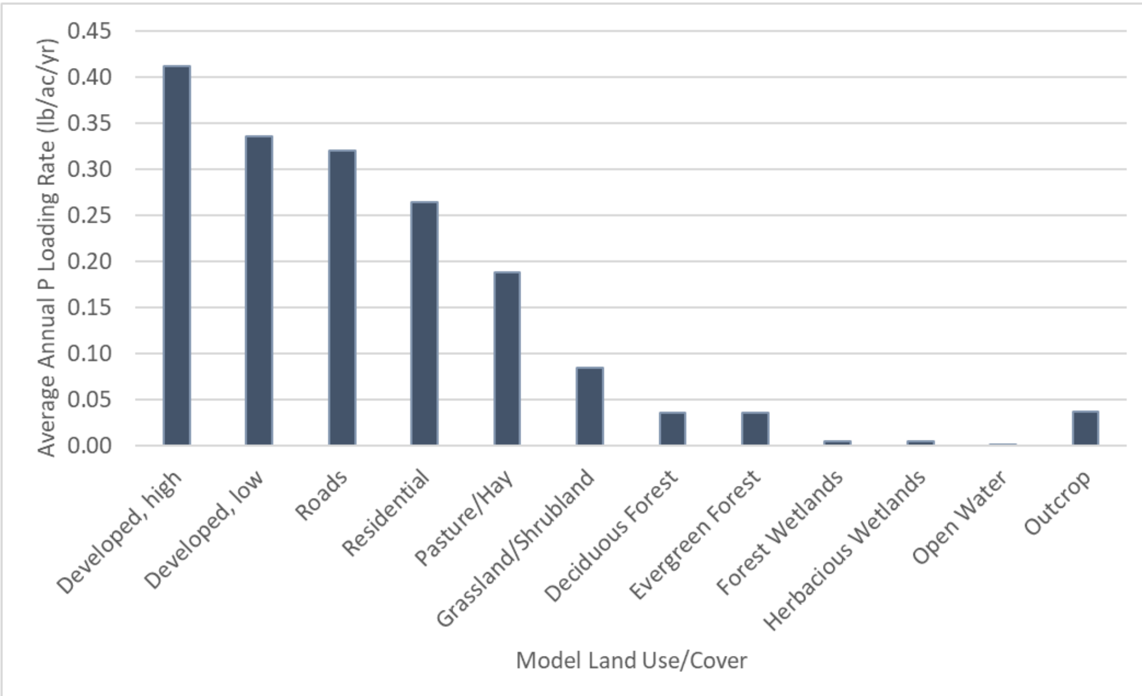

Figure 5-2. Annual average upland TP loading rates by model land use/cover

5.2.2 Point Sources

As discussed in the original report, there are no permitted point sources that discharge to the waterbodies modeled in the Duluth urban area HSPF model.

5.2.3 Calibration and Validation to Observed Nutrients

Nutrients from nonpoint sources are loaded to the stream reaches. Within the stream reaches the model represents the following nutrient species: ammonia, nitrite, nitrate, organic nitrogen, orthophosphate, organic phosphorus, and organic carbon/BOD. The stream reach module simulates instream biogeochemical processes including nutrient uptake and release by plankton and benthic algae, decay of organic matter, nitrification/denitrification, absorption/desorption of nutrients on suspended sediment, and deposition and scour of sediment-stored nutrients.

The nutrient calibration relies on a weight of evidence approach. Upland loading rates are constrained to be in general agreement with literature values (as described above). Model calibration then adjusts parameters to optimize the fit between model predictions and observations at multiple stations throughout the watershed. All water quality samples collected between WY 2009 and WY 2021 were used for the water quality calibration.

Average observed nutrient concentrations are summarized in Table 5-2. Across the sites, average observed concentrations range from 0.348 to 0.805 mg/L for TKN, from 0.169 to 0.353 mg/L for NO_2+NO_3, and from 0.042 to 0.078 mg/L for TP. Comparisons between model predictions and sample observations are made to evaluate the ability of the model to represent conditions in the watershed. Relative error on median and average concentration are listed in Table 5-3 and Table 5-4, respectively. Figures provide an example of the visual comparisons used to calibrate nutrients using monitoring records available at each site. This set of example plots show the N and P calibration at Amity Creek, Tischer Creek, and Keene Creek in Figure 5-3 through Figure 5-20.

As shown by the time series TKN concentration plot for Amity Creek, TKN observation tended to be higher at this location in 2010-2011 compared to 2015-2016; the model does a better job capturing the concentrations observed for the later period of monitoring, in part due to the model land use/cover aligning with this period. As shown in the TP load versus streamflow plot for Amity Creek, simulated concentrations are slightly overpredicted for low flows and slightly underpredicted for high flows. Average observed and simulated TP concentrations are similar at this location at 0.078 and 0.061 mg/L, respectively. The model does a good job of capturing the range in TP and TKN concentrations at Tischer Creek as shown by the time series plots, though some of the smallest observations are not depicted by the model. The model has the poorest fit at Miller Creek. The model tends to overestimate NO_2+NO_3 concentrations at Miller Creek, particularly during streamflows ranging from 5 cfs to about 50 cfs, for example.

Table 5-2. Average observed concentration (mg/L)

Site	HSPF Reach	TKN	$NO_2 + NO_3$	TP
Amity Creek (S001-757)	436+438	0.646	0.344	0.078
Chester Creek (S001-530, S004-953, S008-481, S007-180)	386	0.548	0.353	0.043
Keene Creek (S008-482)	302	0.461	0.317	0.051
Kingsbury Creek (S004-952, S007-005)	272	0.805	0.239	0.058
Merritt Creek (S008-483)	321	0.348	0.286	0.046
Miller Creek (S003-071, S008-484)	330	0.486	0.169	0.042
Tischer Creek (S004-364, S002-480, S007-592)	409+412	0.482	0.255	0.059

Table 5-3. Nutrient calibration summary – relative errors on median concentration

Site	HSPF Reach	TKN	$NO_2 + NO_3$	TP
Amity Creek (S001-757)	436+438	7%	-12%	6%
Chester Creek (S001-530, S004-953, S008-481, S007-180)	386	4%	-13%	42%
Keene Creek (S008-482)	302	42%	-12%	33%
Kingsbury Creek (S004-952, S007-005)	272	-34%	-0.9%	47%
Merritt Creek (S008-483)	321	79%	-8%	43%
Miller Creek (S003-071, S008-484)	330	30%	59%	60%
Tischer Creek (S004-364, S002-480, S007-592)	409+412	-12%	-35%	17%

Table 5-4. Nutrient calibration summary – relative errors on average concentration

Site	HSPF Reach	TKN	$NO_2 + NO_3$	TP
Amity Creek (S001-757)	436+438	-9%	-31%	-21%
Chester Creek (S001-530, S004-953, S008-481, S007-180)	386	-2%	-9%	41%
Keene Creek (S008-482)	302	38%	2%	16%
Kingsbury Creek (S004-952, S007-005)	272	-24%	75%	19%
Merritt Creek (S008-483)	321	78%	4%	28%
Miller Creek (S003-071, S008-484)	330	27%	198%	74%
Tischer Creek (S004-364, S002-480, S007-592)	409+412	-8%	6%	10%

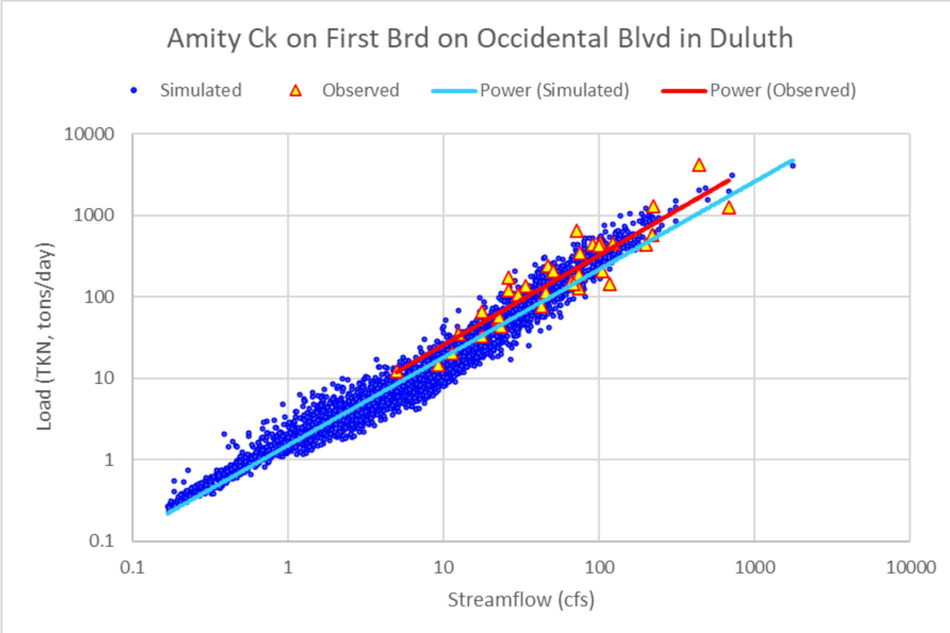

Figure 5-3. Load versus streamflow (TKN) at Amity Creek

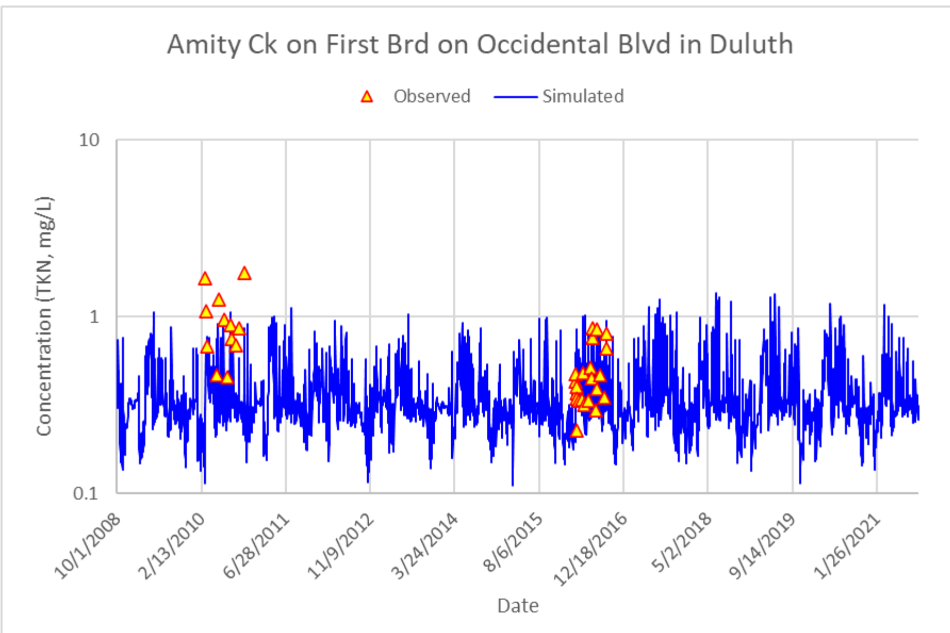

Figure 5-4. Concentration time series (TKN) at Amity Creek

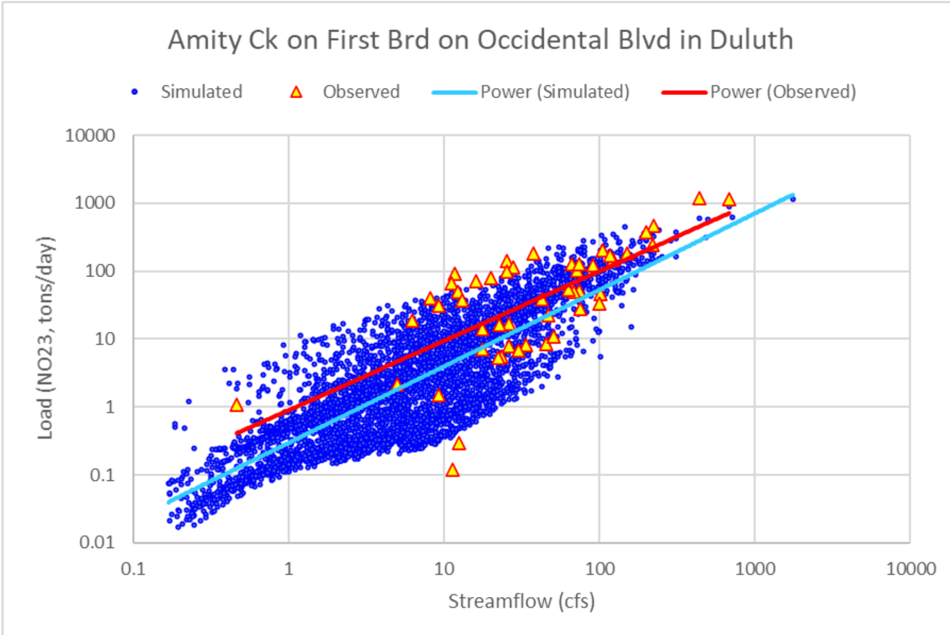

Figure 5-5. Load versus streamflow (NOx) at Amity Creek

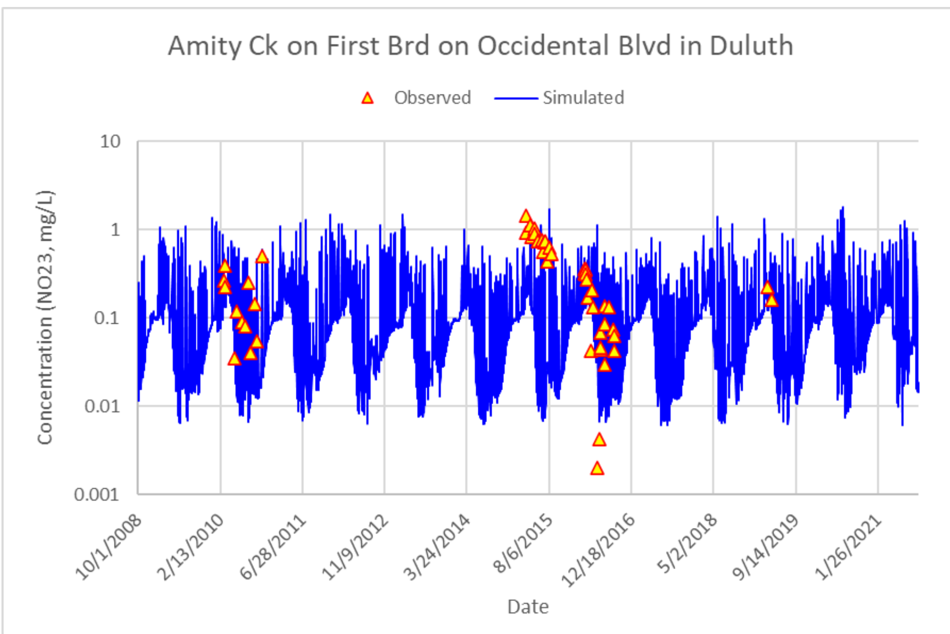

Figure 5-6. Concentration time series (NOx) at Amity Creek

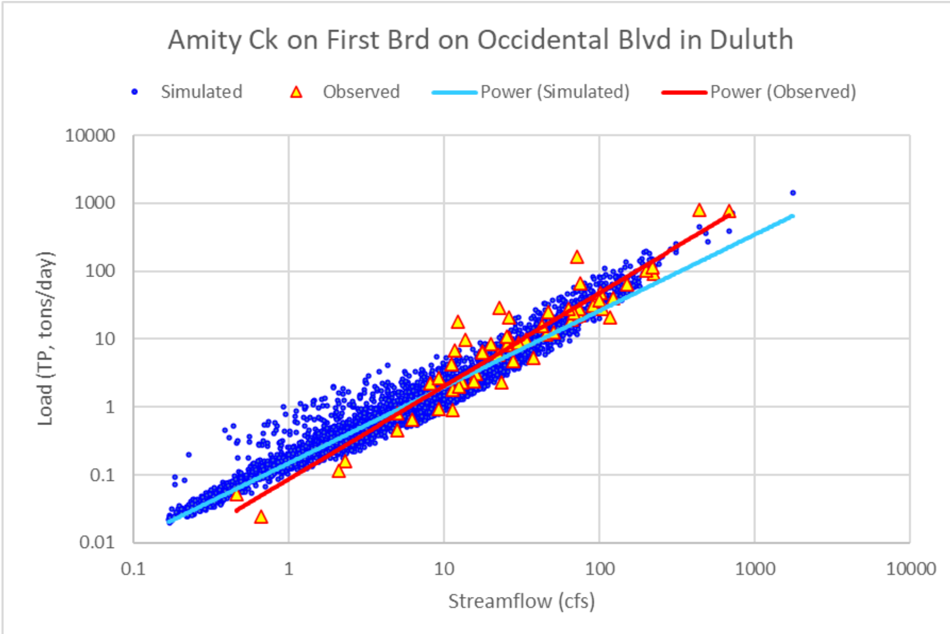

Figure 5-7. Load versus streamflow (TP) at Amity Creek

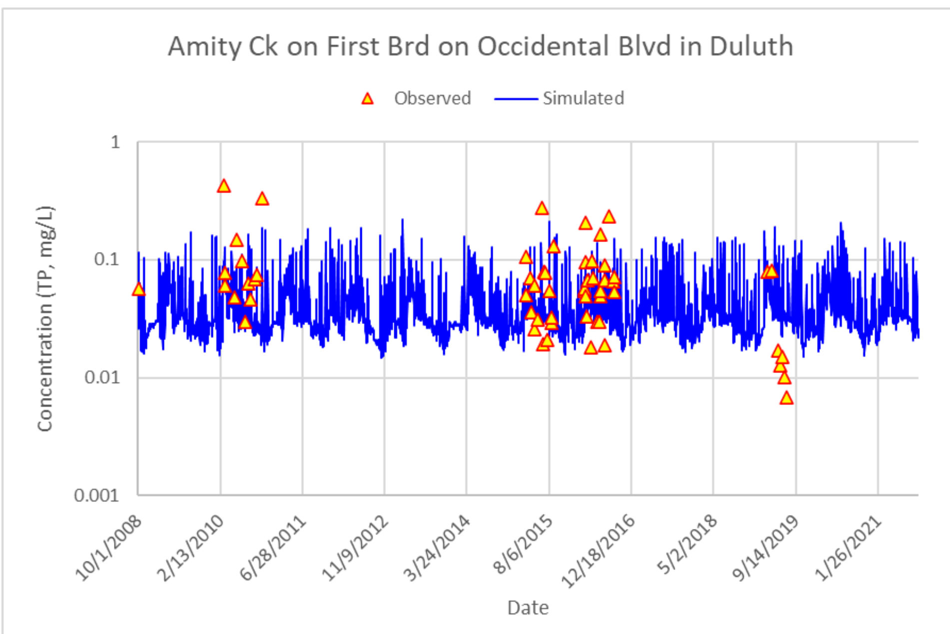

Figure 5-8. Concentration time series (TP) at Amity Creek

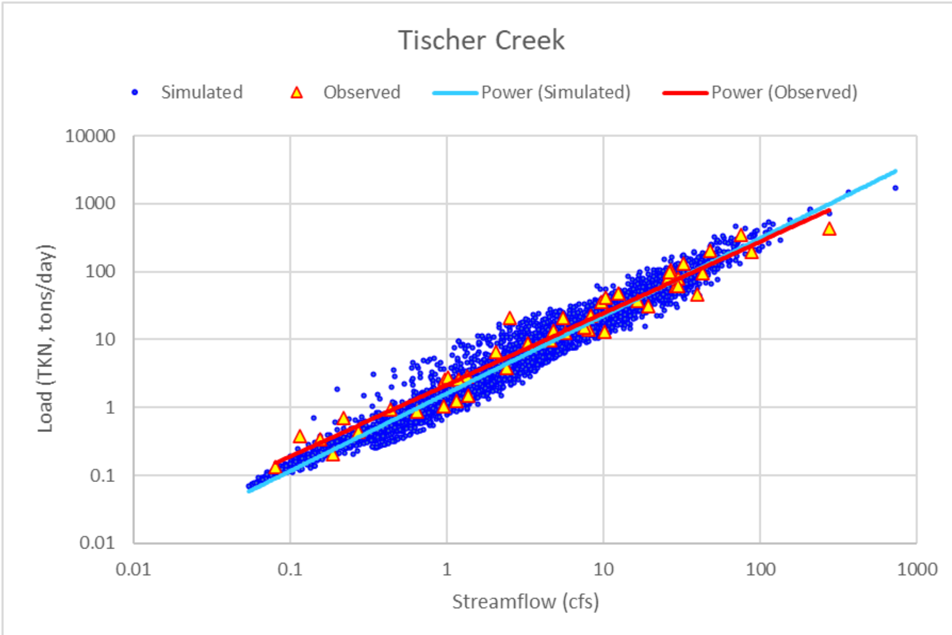

Figure 5-9. Load versus streamflow (TKN) at Tischer Creek

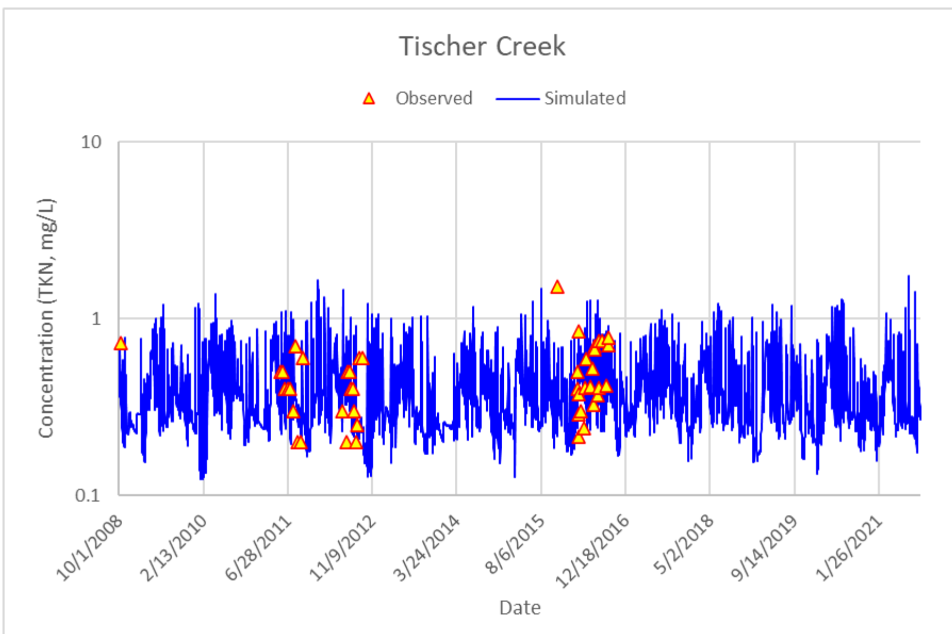

Figure 5-10. Concentration time series (TKN) at Tischer Creek

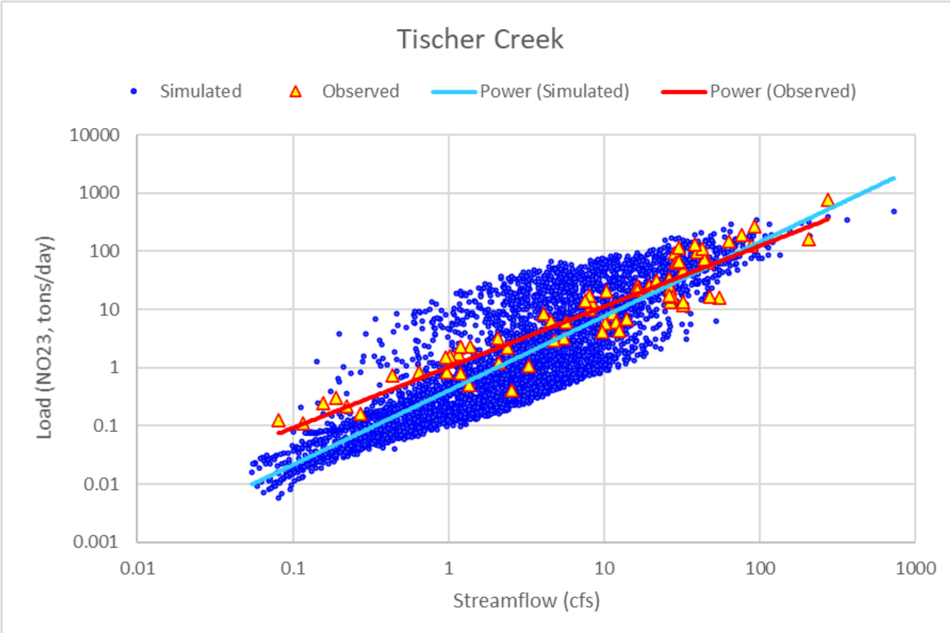

Figure 5-11. Load versus streamflow (NOx) at Tischer Creek

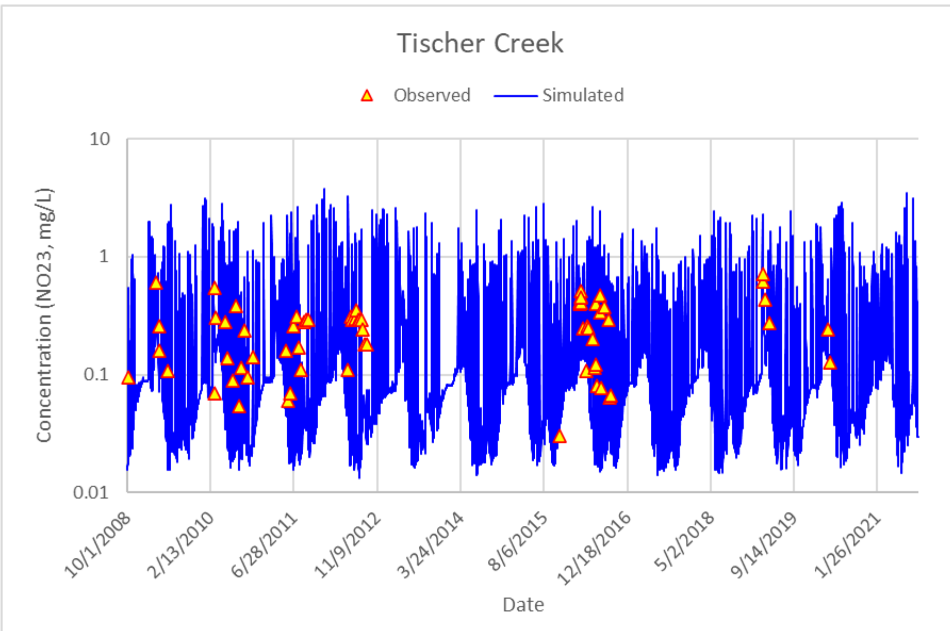

Figure 5-12. Concentration time series (NOx) at Tischer Creek

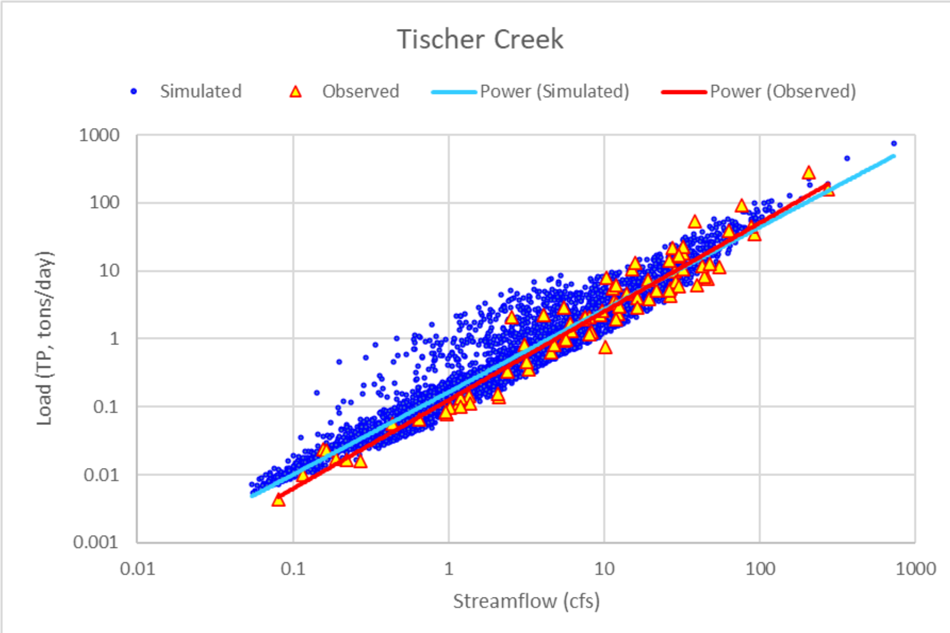

Figure 5-13. Load versus streamflow (TP) at Tischer Creek

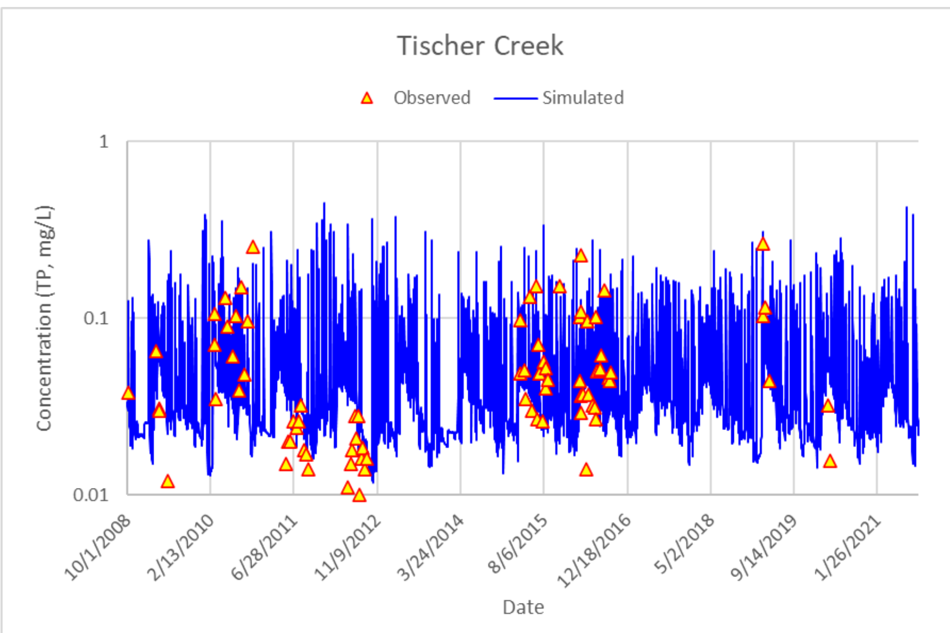

Figure 5-14. Concentration time series (TP) at Tischer Creek

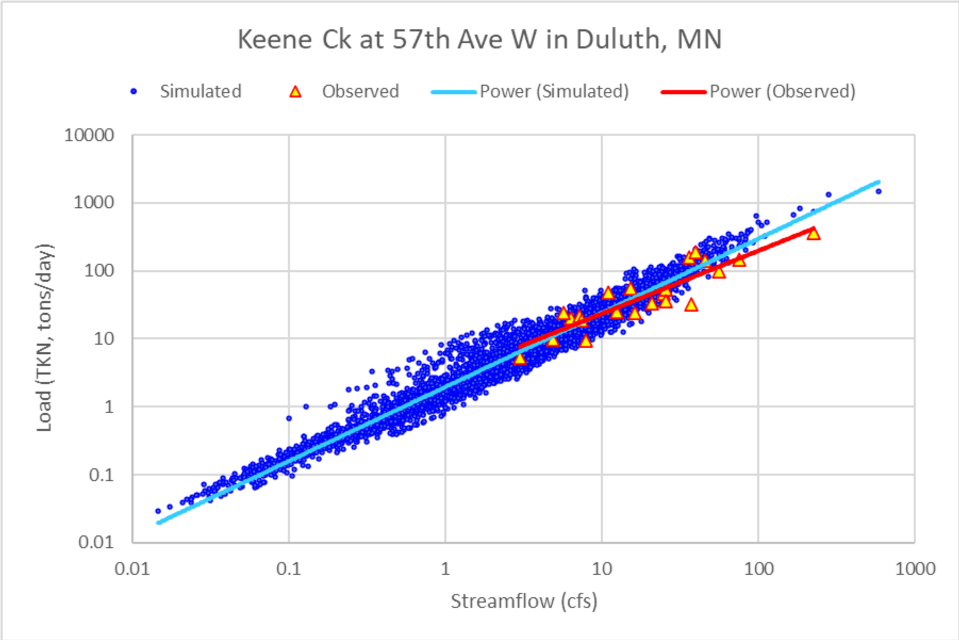

Figure 5-15. Load versus streamflow (TKN) at Keene Creek

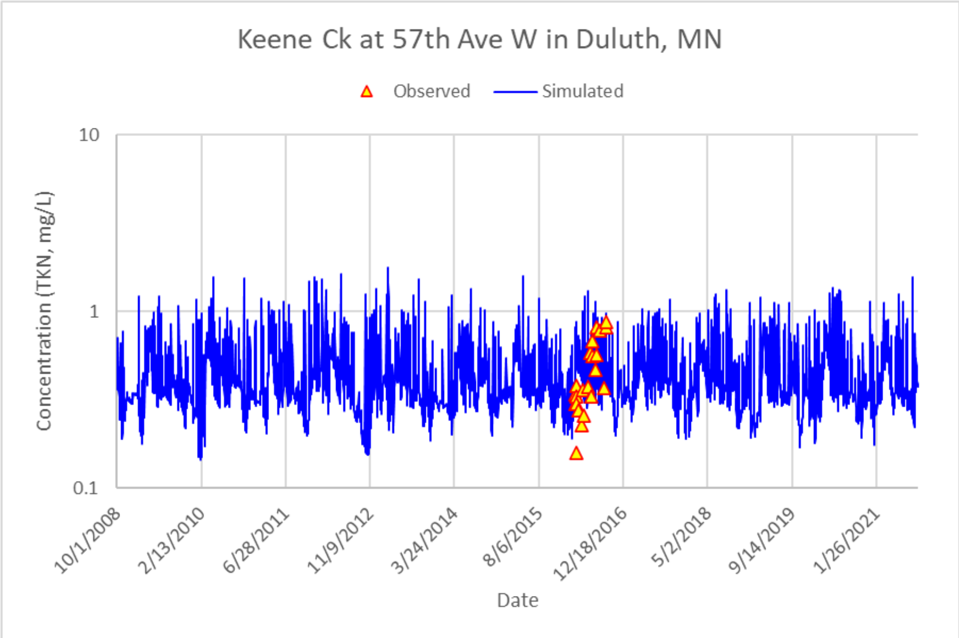

Figure 5-16. Concentration time series (TKN) at Keene Creek

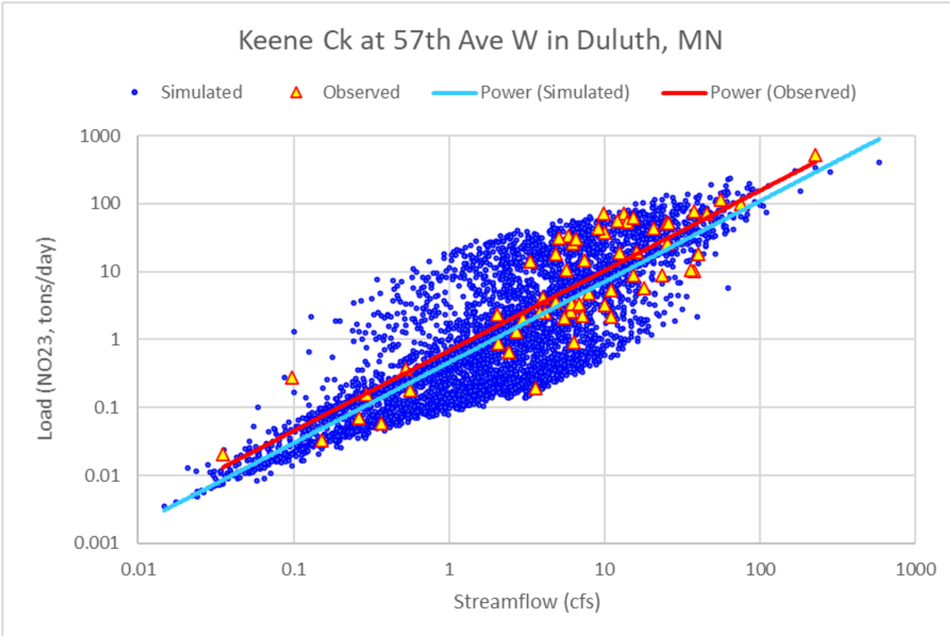

Figure 5-17. Load versus streamflow (NOx) at Keene Creek

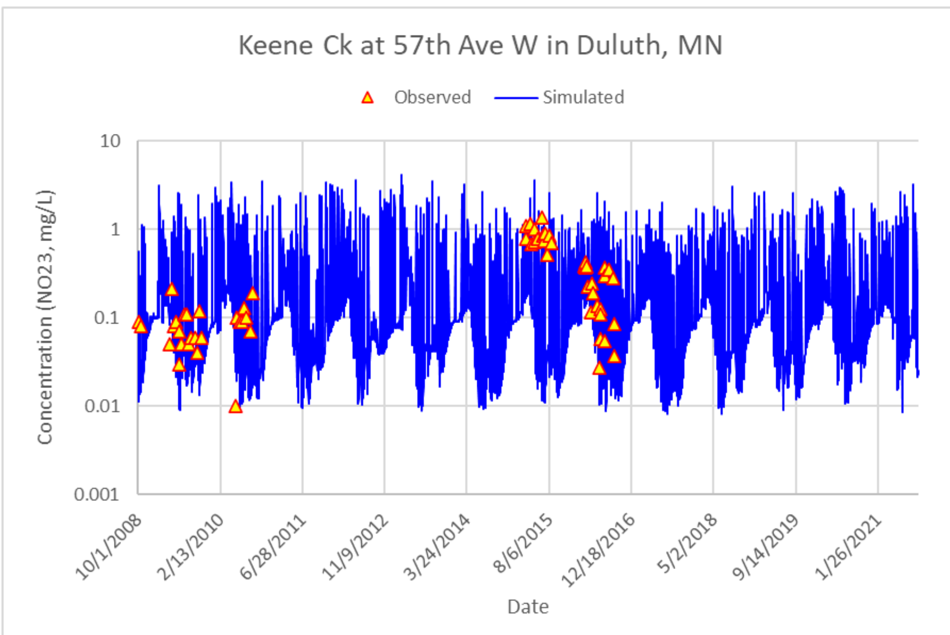

Figure 5-18. Concentration time series (NOx) at Keene Creek

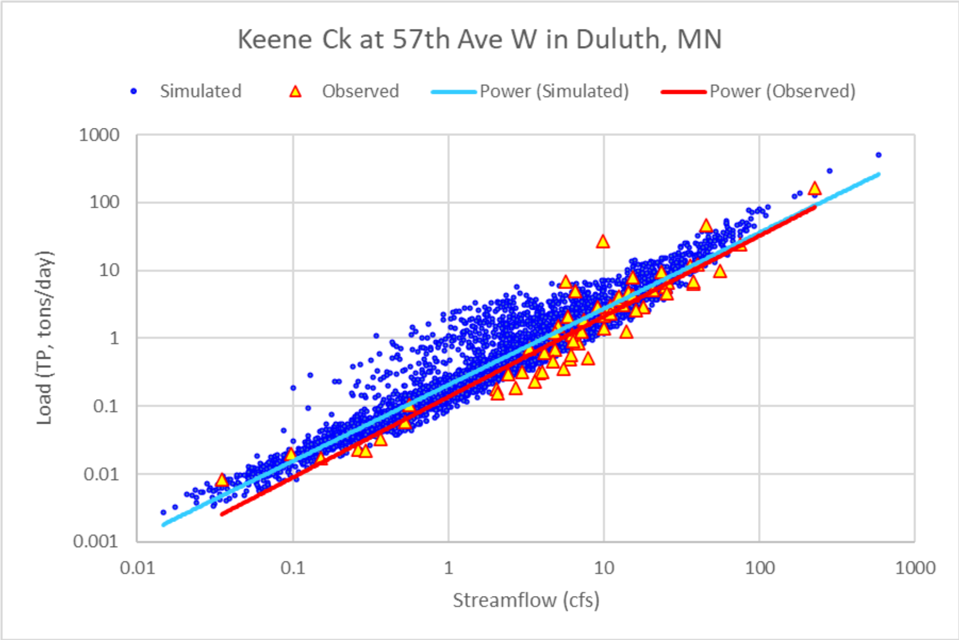

Figure 5-19. Load versus streamflow (TP) at Keene Creek

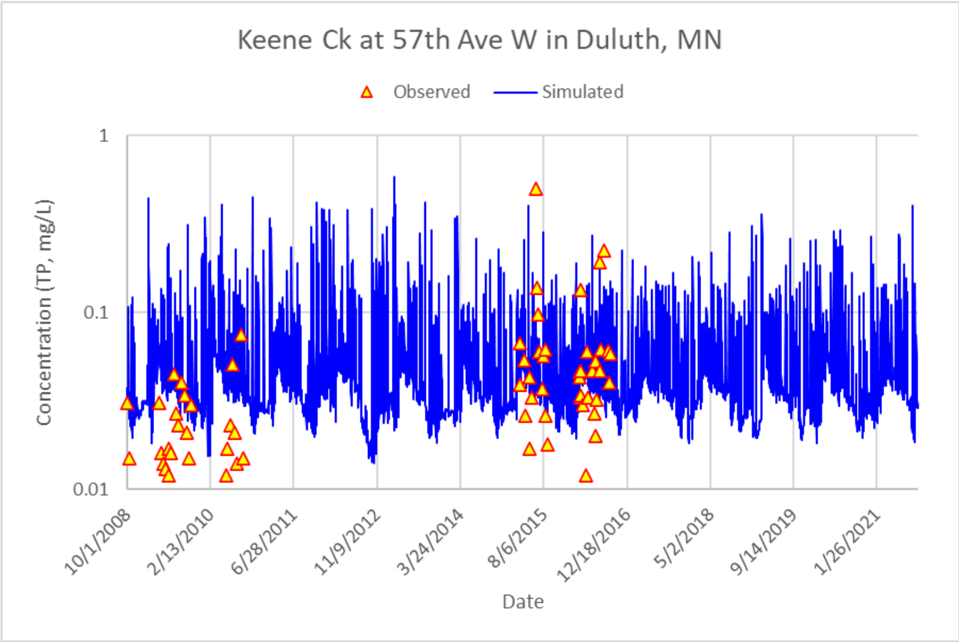

Figure 5-20. Concentration time series (TP) at Keene Creek

5.2.4 Organic Carbon

The Duluth urban area HSPF model will be used to develop a mercury TMDL for the St. Louis River estuary and harbor. Dissolved organic carbon (DOC) will serve as a surrogate for upland transport of mercury. Thus, available organic carbon records were used to calibrate DOC and total organic carbon (TOC). The RQUAL module of HSPF simulates dead refractory organic carbon and total inorganic carbon, and total organic carbon can be computed as the dead refractory organic carbon plus the carbon hidden in phytoplankton and in BOD. HSPF does not split organic carbon into dissolved and particulate portions. Therefore, the model was calibrated such that phytoplankton associated organic carbon is assumed as particulate organic carbon whereas the organic carbon in BOD and dead refractory organic carbon were considered as the dissolved portion. A summary of simulated 5th percentile, median, and 95th percentile DOC concentrations is in Table 5-5. Only seven DOC samples were available, all collected along Lester River in September 2015; on that day of sampling DOC ranged from 12 mg/L to 33.6 mg/L across the sites. Data were thus quite limited both spatially and temporally, nonetheless, the observed concentration range served as a guide for model calibration. Time series plots are provided for Lester River at Jean Duluth Road (S007-815) and Lester River at Lismore Road / CR-43 (S007-816).

Table 5-5. Simulated DOC concentrations (mg/L)

Site	Observed DOC Concentration (sample count)	5th Percentile Concentration	Median Concentration	95th Percentile Concentration
Kingsbury Creek at Lake Superior Zoo	NA (n=0)	6.3	10.8	22.6
Keene Creek at S. 57th Ave. W	NA (n=0)	6.5	10.5	21.0
Merritt Creek at Grand Ave.	NA (n=0)	6.3	10.0	20.0
Miller Creek at S. 24th Ave. W	NA (n=0)	5.6	9.4	21.7
Chester Creek at Wallace Ave.	NA (n=0)	6.8	11.2	22.1
Tischer Creek at Wallace Ave.	NA (n=0)	5.4	9.1	19.3
Amity Creek at Duluth, Occidental Blvd	NA (n=0)	5.3	9.2	18.7
Lester River above Superior St.	NA (n=0)	3.9	7.8	20.2
Lester River near Duluth, CSAH10	14.4 (n=2)	3.6	8.5	22.0
Lester River just upstream of Cnty Rd 293	15.1 (n=1)	4.8	9.9	23.2
Lester River at Jean Duluth Rd /CR-37	19.6 (n=1)	5.9	11.5	24.3
Lester River at Lismore Rd / CR-43	12.8 (n=1)	6.1	11.8	24.9
Lester River at Arnold Rd / CR-675	33.6 (n=1)	6.2	12.4	25.7
Unnamed Lester River Tributary at Zimmerman Rd	19.1 (n=1)	6.3	14.0	26.1
Mission Creek nr Fond du Lac, 1 mi MN23	NA (n=0)	7.0	10.8	19.8
Buckingham Creek at Duluth, 0.4mi us Skyline Parkway	NA (n=0)	6.4	10.5	19.8
East Branch Amity Creek at Duluth, 1.8 mi ds of CSAH37	NA (n=0)	5.8	9.9	21.1

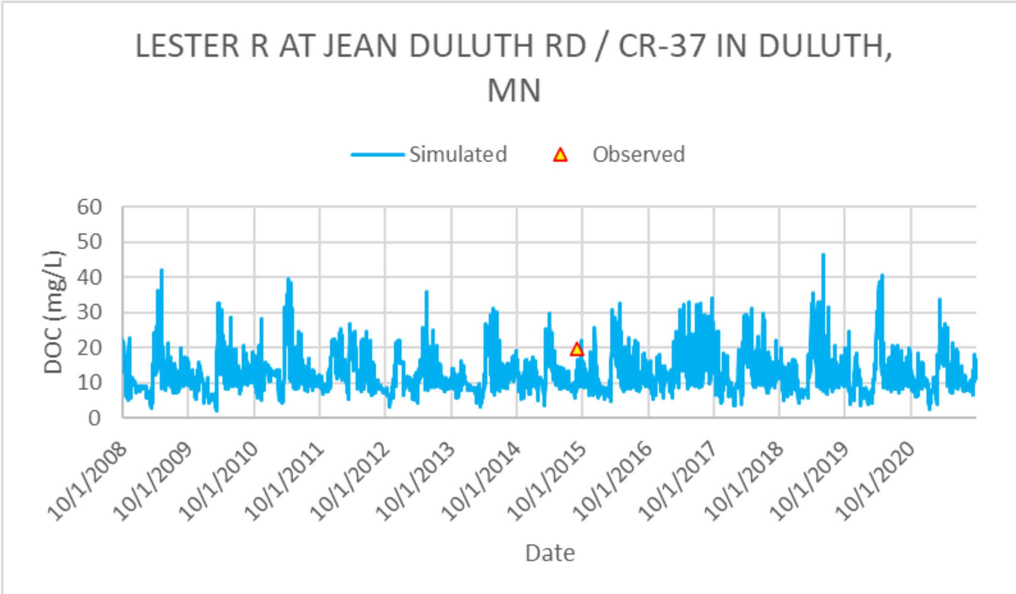

Figure 5-21. Time series of observed and simulated DOC concentration at Lester River at Jean Duluth Road (S007-815)

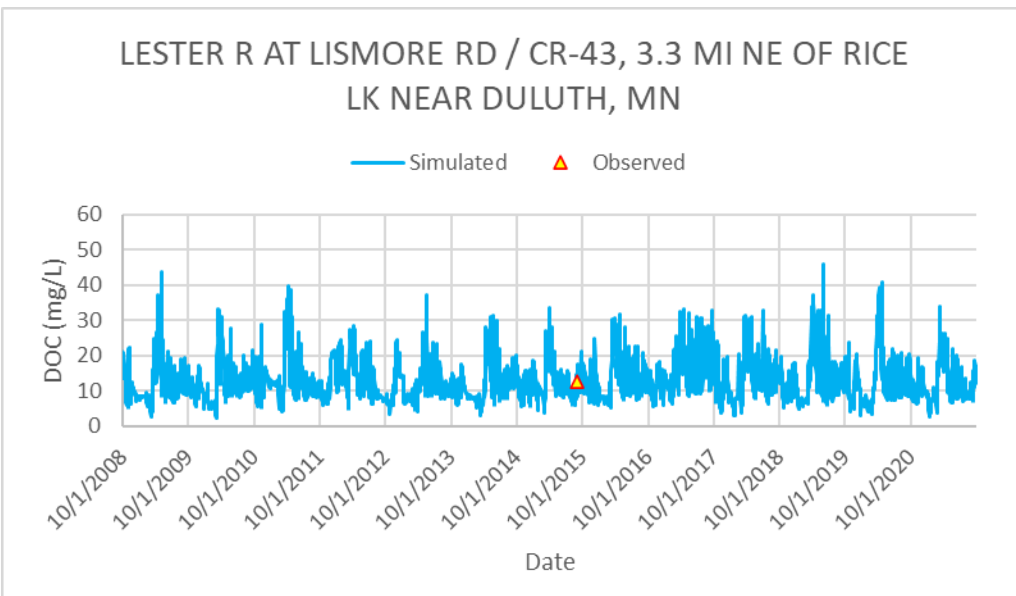

Figure 5-22. Time series of observed and simulated DOC concentration at Lester River at Lismore Road (S007-816)

6.0 SUMMARY AND RECOMMENDATIONS

The HSPF model of the Duluth urban area was extended to simulate conditions through WY 2021. Weather time series were derived from local station data and publicly available gridded weather datasets for the extension period consistent with the previous iteration of the HSPF model. In addition, time series inputs for wet and dry atmospheric deposition of N were extended in time. There are no permitted point sources in the HSPF model. The land use/cover component of model HRUs was also refined to depict more recent conditions (i.e., updating from NLCD 2011 to NLCD 2016).

Following the model updates and extension, the model was recalibrated for hydrology and water quality. The hydrology calibration collectively evaluated the simulation of snow, evapotranspiration, and streamflow. Metrics for the hydrologic calibration (e.g., NSEs) were similar to that of the previous iteration of the model following the extension and recalibration. The overall hydrologic calibration was successful and serves as a solid foundation for water quality simulation. The water quality calibration was evaluated and tuned with instream monitoring records as described in Sections 4.0 and 5.0. In addition to typical variables, the model calibration also focused on DOC. The HSPF model is going to be used in the development of a mercury TMDLs for the St. Louis River Harbor/Estuary. Past research has found that water column concentrations of mercury and methylmercury are strongly correlated with DOC in the watershed, thus, DOC will serve as a landscape transport surrogate for mercury. To support that upcoming phase of work, available DOC records were used for model calibration, however, records were very limited in the study area.

7.0 REFERENCES

AQUA TERRA Consultants. 2012. Modeling Guidance for BASINS/HSPF Applications under the MPCA One Water Program. Prepared for Minnesota Pollution Control Agency by AQUA TERRA Consultants, Mountain View, CA.

Bicknell, B.R., J.C. Imhoff, J.L. Kittle, Jr., T.H. Jobes, P.B. Duda, and A.S. Donigian, Jr. 2014. HSPF Version 12.4 User's Manual. National Exposure Research Laboratory, Office of Research and Development, U.S. Environmental Protection Agency, Athens, GA.

Carroll, T., D. Cline, G. Fall, A. Nilsson, L. Li, and A. Rost. 2001. NOHRSC Operations and the Simulation of Snow Cover Properties for the Conterminous U.S. Proceedings of the 69th Annual Meeting of the Western Snow Conference, pp. 1-14.

Daly, C., M. Halbleib, J.I. Smith, W.P. Gibson, M.K. Doggett, G.H. Taylor, J. Curtis, and P.P. Pasteris. 2008. Physiographically sensitive mapping of climatological temperature and precipitation across the conterminous United States. *International Journal of Climatology*, doi:10.1002/joc.1688.

Donigian, A.S. Jr., and J.T. Love. 2003. Sediment Calibration Procedures and Guidelines for Watershed Modeling. Presented at the Water Environment Federation Total Maximum Daily Load Conference, November 16–19, 2003, Chicago, IL.

Donigian, A.S., Jr. 2000. HSPF Training Workshop Handbook and CD. Lecture #19. Calibration and Verification Issues. Prepared for and presented to the U.S. Environmental Protection Agency, Office of Water, Office of Science and Technology, Washington, DC.

Donigian, A.S., Jr., J.C. Imhoff, B.R. Bicknell, and J.L. Kittle, Jr. 1984. Application Guide for Hydrological Simulation Program – FORTRAN (HSPF). EPA-600/3-84-965. U.S. Environmental Protection Agency, Environmental Research Laboratory, Athens, GA.

Duda, P.B., P.R. Hummel, A.S. Donigian, Jr., and J.C. Imhoff. 2012. BASINS/HSPF: Model use, calibration, and validation. *Transactions of the ASABE*, 55(4): 1523-1547.

Ebrahimian, A. and B.N. Wilson. 2015. Determination of Effective Imprevious Area In Urban Watersheds. St. Paul: Minnesota Department of Transportation.

Kohler M.A., Nordenson T.J., Fox W.E. 1955. Evaporation from Pans and Lakes. Research Paper No. 38, U.S. Weather Bureau.

Mitchell, K. E., et al. 2004. The multi-institution North American Land Data Assimilation System (NLDAS): Utilizing multiple GCIP products and partners in a continental distributed hydrological modeling system. *J. Geophys. Res.*, 109, D07S90.

Moriasi, D.N., J.G. Arnold, M.W. Van Liew, R.L. Bingner, R.D. Harmel, and T.L. Veith. 2007. Model evaluation guidelines for systematic quantification of accuracy in watershed simulations. *Transactions of the ASABE*, 50(3): 885-900.

Nash, J.E. and J.V. Sutcliffe. 1970. River flow forecasting through conceptual models part I – A discussion of principals. *Journal of Hydrology*, 10(3): 282-290.

Penman H.L. 1948. Natural Evaporation from Open Water, Bare Soil, and Grass. Proceedings of the Royal Society of London, Ser. A, 193(1032):120-145.

Sanford, W.E. and D.L. Selnick. 2013. Estimation of evapotranspiration across the conterminous United States using a regression with climate and land-cover data. *Journal of the American Water Resources Association*, 49(1): 217-230.

Senay, G.B., Bohms, Stefanie, Singh, R.K., Gowda, P.H., Velpuri, N.M., Alemu, Henok, and Verdin, J.P. 2013. Operational evapotranspiration modeling using remote sensing and weather datasets—A new parameterization for the SSEB ET approach: *Journal of the American Water Resources Association*, v. 49, no. 3, p. 577–591.

Senay, G.B., Budde, M.E., and Verdin, J.P. 2011a. Enhancing the Simplified Surface Energy Balance (SSEB) approach for estimating landscape ET-Validation with the METRIC model: *Agricultural Water Management*, v. 98, no. 4, p. 606–618.

Senay, G.B., Leake, S.A., Nagler, P.L., Artan, G.A., Dickinson, J.E., Cordova, J.T. and Glenn, E.P. 2011b. Estimating basin scale evapotranspiration (ET) by water balance and remote sensing methods: Hydrological Processes, v. 25, p. 4,037–4,049.

Senay, G.B., Budde, M.E., Verdin, J.P., and Melesse, A.M. 2007. A coupled remote sensing and simplified surface energy balance approach to estimate actual evapotranspiration from irrigated fields: Sensors, v. 7, p. 979–1,000.SSURGO: Digital soils data produced and distributed by the Natural Resources Conservation Service (NRCS) - National Cartography and Geospatial Center (NCGC). http://www.nrcs.usda.gov/wps/portal/nrcs/detail/soils/survey/?cid=nrcs142p2_053627

Sutherland. 1995. *Methodology for Estimating the Effective Imprevious Area of Urban Watersheds* . Watershed Protection Technique, Vol 2, No.1.

Tetra Tech. 2020. Gridded Weather Data Processing (MET)Tool: User Guide for Hydrologic Simulation Program FORTRAN (HSPF) Application. Prepared for Minnesota Pollution Control Agency by Tetra Tech, Research Triangle Park, North Carolina.

Tetra Tech. 2019. Duluth Urban WRASP HSPF Model Report (REVISED). Prepared for Minnesota Pollution Control Agency by Tetra Tech, Research Triangle Park, North Carolina.

University of Minnesota. 2019. Retrieved from Libraries Digital Conservancy: https://conservancy.umn.edu/handle/11299/57196 Prepared for Minnesota Pollution Control Agency by Tetra Tech, Research Triangle Park, North Carolina.

USEPA. 2006. BASINS Technical Note 8: Sediment Parameter and Calibration Guidance for HSPF. Office of Water, U.S. Environmental Protection Agency, Washington, DC.

USEPA. 2000. Estimating Hydrology and Hydraulic Parameters for HSPF. BASINS Technical Note 6, EPA-823-R00-012. Office of Water, U.S. Environmental Protection Agency, Washington, DC.

Velpuri, N.M., G.B. Senay, R.K. Singh, S. Bohms, and J.P. Verdin. 2013. A comprehensive evaluation of two MODIS evapotranspiration products over the conterminous United States: Using point and gridded FLUXNET and water balance ET. *Remote Sensing of Environment*, 139: 35-49.

Wischmeier, W. H. and D. D. Smith. 1978. Predicting Rainfall Erosion Losses: A Guide to Conservation Planning. Agricultural Handbook, 537. U.S. Governmentl Printing Office, Washington, DC.